END
DATE
FILMED

3 82

DTIC

1.0

2.8 2.5

3.2 2.2

3.6

4.0 2.0

1.1

1.8

1.25 1.4 1.6

MICROCOPY RESOLUTION TEST CHART

NATIONAL BUREAU OF STANDARDS 1963 A

SECURITY CLASSIFICATION OF THIS PAGE (When Data Entered)

REPORT DOCUMENTATION PAGE		READ INSTRUCTIONS BEFORE COMPLETING FORM
1. REPORT NUMBER ONR Tr-32	2. GOVT ACCESSION NO. AD-A110	3. RECIPIENT'S CATALOG NUMBER 087
4. TITLE (and Subtitle) "Chemically Derivatized Semiconductor Photoelectrodes"		5. TYPE OF REPORT & PERIOD COVERED Interim Technical Report
		6. PERFORMING ORG. REPORT NUMBER
7. AUTHOR(s) Mark S. Wrighton		8. CONTRACT OR GRANT NUMBER(s) N00014-75-C-0880
9. PERFORMING ORGANIZATION NAME AND ADDRESS Department of Chemistry Massachusetts Institute of Technology Cambridge, Massachusetts 02139		10. PROGRAM ELEMENT, PROJECT, TASK AREA & WORK UNIT NUMBERS NR 051-579
11. CONTROLLING OFFICE NAME AND ADDRESS Office of Naval Research Department of the Navy Arlington, Virginia 22217		12. REPORT DATE January 4, 1982
		13. NUMBER OF PAGES 44
14. MONITORING AGENCY NAME & ADDRESS(if different from Controlling Office)		15. SECURITY CLASS. (of this report) UNCLASSIFIED
		15a. DECLASSIFICATION/DOWNGRADING SCHEDULE

16. DISTRIBUTION STATEMENT (of this Report)

Distribution unlimited; approved for public release; reproduction is permitted for any purpose of the United States Government

17. DISTRIBUTION STATEMENT (of the abstract entered in Block 20, if different from Report)

Distribution of this document is unlimited

JAN 2 6 1932

A

18. SUPPLEMENTARY NOTES

Prepared for publication in ACS Symposium Series volume, "Chemical Modification of Surfaces"

19. KEY WORDS (Continue on reverse side if necessary and identify by block number)
photoelectrochemistry, derivatization, semiconductors, photoelectrodes

01 26 82 051

20. ABSTRACT (Continue on reverse side if necessary and identify by block number)

Highlights of research results from the chemical derivatization of n-type semiconductors with (1,1'-ferrocenediyl)dimethylsilane, I, and its dichloro analogue, II and from the derivatization of p-type semiconductors with {N,N'-bis[3-trimethoxysilyl)propyl]-4,4'-bipyridinium}dibromide, III are presented. Research Shows that molecular derivatization with II can be used to suppress photoanodic corrosion of n-type Si; derivatization of p-type Si with III can be used to improve photoreduction kinetics for horseheart ferricytochrome c; →
(continued on reverse)

DD, FORM 1473, JAN 73   EDITION OF 1 NOV 65 IS OBSOLETE
S/N 0102-014-6601 |

220 007

derivatization of p-type Si with (III) followed by incorporation of Pt(0) improves photoelectrochemical H_2 production efficiency. Strongly interacting reagents can alter semiconductor/electrolyte interface energetics and surface state distributions as illustrated by n-type WS_2/I^- interactions and by differing etch procedures for n-type CdTe.

OFFICE OF NAVAL RESEARCH

CONTRACT N00014-75-C-0880

Task No. NR 051-579

TECHNICAL REPORT NO. 32

"CHEMICALLY DERIVATIZED SEMICONDUCTOR PHOTOELECTRODES"

by

Mark S. Wrighton

Department of Chemistry
Massachusetts Institute of Technology
Cambridge, Massachusetts   02139

January 4, 1982

CHEMICALLY DERIVATIZED SEMICONDUCTOR PHOTOELECTRODES

MARK S. WRIGHTON, DEPARTMENT OF CHEMISTRY, MASSACHUSETTS
INSTITUTE OF TECHNOLOGY, CAMBRIDGE, MASSACHUSETTS 02139 U.S.A.

Highlights of research results from the chemical
derivatization of n-type semiconductors with (1,1'-
ferrocenediyl)dimethylsilane, I, and its dichloro
analogue, II, and from the derivatization of p-type
semiconductors with {N,N'-bis[3-trimethoxysilyl)-
propyl]-4,4'-bipyridinium}dibromide, III are
presented. Research shows that molecular deriva-
tization with II can be used to suppress photo-
anodic corrosion of n-type Si; derivatization of
p-type Si with III can be used to improve
photoreduction kinetics for horseheart ferricyto-
chrome c; derivatization of p-type Si with III
followed by incorporation of Pt(0) improves
photoelectrochemical H_2 production efficiency.
Strongly interacting reagents can alter semicon-
ductor/electrolyte interface energetics and surface
state distributions as illustrated by n-type WS_2/I^-
interactions and by differing etch procedures for
n-type CdTe.

Derivatization of the surface of semiconductor photo-
electrodes may be useful in suppressing corrosion reactions of
the electrode (1-5), accelerating the rate of desired redox
processes (6-8), measuring rate constants for reactions of
surface-confined redox reagents (9,10), bringing about changes in
the energetics of the semiconductor/electrolyte interface(11,12),
and altering the distribution of surface states associated with
the semiconductors.(13,14) Work in this laboratory has concerned
the study of n-type semiconductor photoelectrode materials such
as Si, Ge, and GaAs derivatized with reagents based on ferrocene
such as those represented by I and II. Work with p-type
semiconductor photoelectrode materials such as Si concerns the
use of the N,N'-dialkyl-4,4'-bipyridinium-based derivatizing

reagent represented by III. The results from these studies do

I

II

III
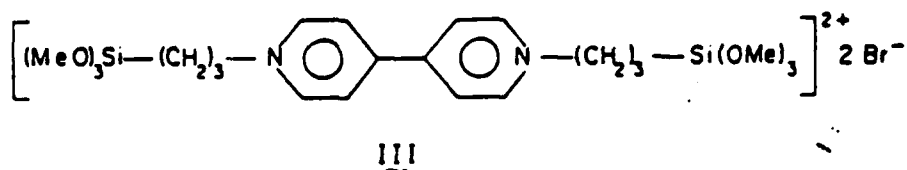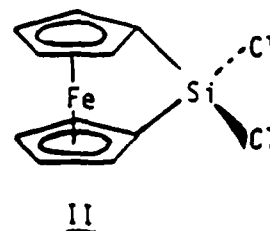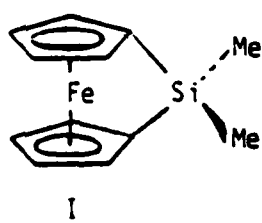
suggest that surface derivatization may be useful in certain
practical and fundamental applications. The highlights of the
studies to date along with the limitations associated with
chemical derivatization will be summarized in this article.

## Suppression of Photoanodic Corrosion of N-Type Semiconductors

All n-type semiconductors are thermodynamically unstable
when irradiated with supra band gap energy light in the presence
of liquid electrolytes.(15-17) However, it is well known that
durable n-type semiconductor/electrolyte/redox couple
combinations do exist.(18,19) For example, it has been found
that n-type Si, that can undergo surface photooxidation according
to equation (1) can be protected from corrosion.(20) In equation

$$Si + 2xh^+ + xH_2O \longrightarrow SiO_x + 2xH^+ \qquad (1)$$

(1) h^+ represents the photogenerated minority carrier (hole) that
comes to the semiconductor surface under depletion conditions as
illustrated in Scheme I. If the oxidative decomposition of Si
proceeds too far the SiO_x thickness ultimately blocks the flow of
current and useful photoelectrochemical effects cease. The oxi-
dative decomposition can be suppressed if some redox active
species A can compete for the h^+, equation (2). Since the photo-

$$A + h^+ \longrightarrow A^+ \qquad\qquad (2)$$

anodic decomposition of semiconductors is generally a multistep
process it would seem that fast, one-electron reductants would be
able to completely suppress photoanodic corrosion by neutralizing
the h^+ before the decomposition process can begin. A priori the
species A should have fast heterogeneous electron transfer
kinetics, be durable in both the A and A^+ oxidation levels, be
optically transparent, be present at high effective concen-
tration, and have an $E^{\circ\prime}(A^+/A)$ that gives a good efficiency from
the point of view of output photovoltage, E_V. Referring to
Scheme I, E_V for the photoanode is the extent to which the
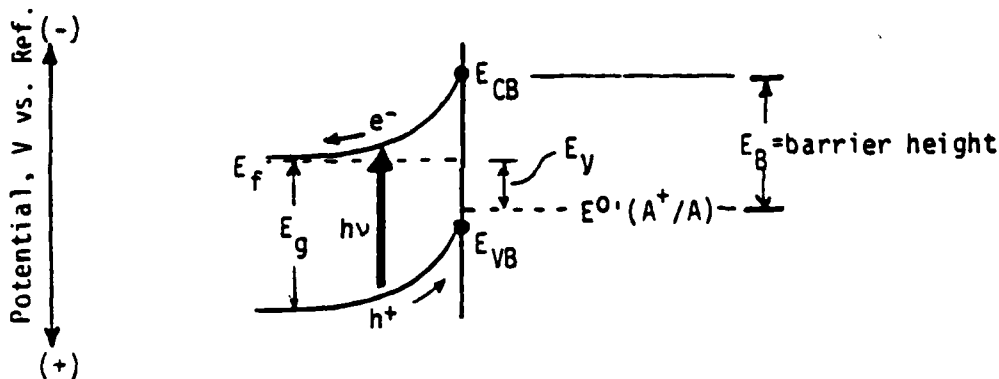
Scheme I. Interface energetics for an n-type semiconductor under
illumination giving an uphill oxidation of A to A^+ to the extent of
of E_V. Generally, the desired oxidation is only competitive with the
anodic decomposition of the semiconductor. In the diagram E_f represents
the electrode potential; E_{CB} the bottom of the conduction band; and E_{VB}
the top of the valence band. At open-circuit $E_V = E_B$.

oxidation occurs at a potential more negative than the E_{redox} of
the solution. Concerning n-type Si it was found that EtOH/0.1 M
[n-Bu$_4$N]ClO$_4$ solutions containing A = ferrocene and A^+ = ferri-
cenium result in a constant output of electrical energy from an
illuminated photoelectrochemical device configured as in Scheme
II.(20) The ferrocene captures the photogenerated h^+ at a rate
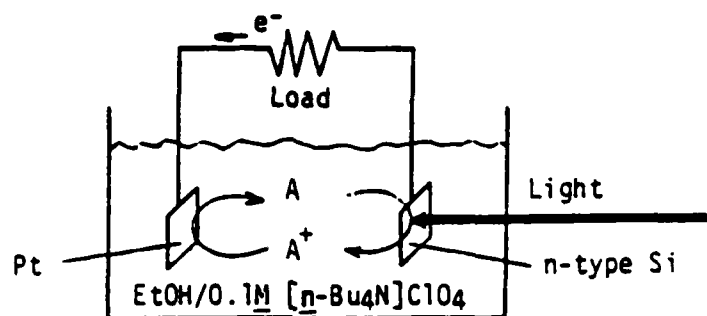
Scheme II. Representation of an n-type Si photoanode-based cell for the conversion of light to electricity.

that precludes photoanodic corrosion of the n-type Si. The purpose in using EtOH solvent is to remove as much H_2O as possible from the solvent to reduce the importance of the photo-oxidation process (1).

The experiments with the n-type Si/ferrocene in EtOH/0.1 M [n-Bu$_4$N]ClO$_4$ prompted the initial work in this laboratory on the surface derivatization of photoelectrodes. The ferrocene-based reagent, II, was anchored to the surface according to equation (3).(1-3) The resulting polymer confronts the n-type Si
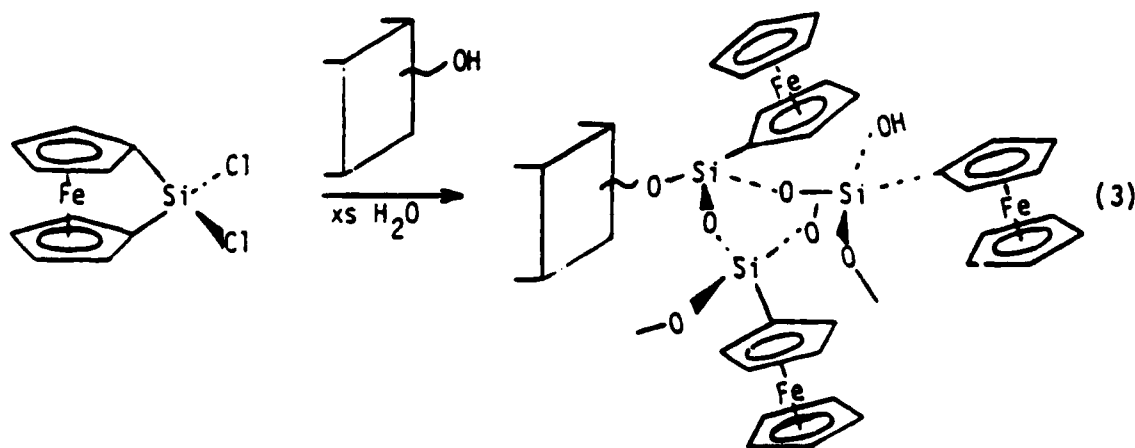
surface with a high effective concentration of the reducing agent A. The important fact with respect to suppressing electrode corrosion was the finding that n-type Si functionalized with II is capable of being used in aqueous electrolyte solution under conditions where the naked (non-derivatized) electrode suffers photodecomposition at a rate that precludes any reproducible photoelectrochemistry. When the reagent A is confined to the photoelectrode surface sustained current flow results from the sequence represented by equations (4)-(5) where the photo-

$$\text{surface-A} + h^+ \xrightarrow{k_4} \text{surface-A}^+ \qquad (4)$$

$$\text{surface-A}^+ + B \xrightarrow{k_5} \text{surface-A} + B^+ \qquad (5)$$

generated, surface-confined oxidant, A^+, reacts heterogeneously with a solution species B to form B^+ and reduce A^+ to A.(2,3,9, 10) For the surfaces resulting from treatment with II the surface oxidant is a ferricenium derivative and anything oxidizeable with ferricenium should be oxidizeable with a photoanode derivatized with II. A number of aqueous species B have been photooxidized using n-type Si derivatized with II including $Ru(NH_3)_6^{2+}$, $Fe(CN)_6^{4-}$, $Co(2,2'-bipyridine)_3^{2+}$, and I^-.(2,3,9,10) In every case the photocurrent is relatively constant compared to that from a naked n-type Si photoanode. Quite interestingly, no aqueous redox additive has been demonstrated to suppress photooxidation of Si to the extent that can be achieved using the surface derivatization procedure. However, even electrodes functionalized with I do not last indefinitely in aqueous solution. Typically, naked n-type Si photoanodes give a photo-current that declines by >90% in <5 min under conditions where the derivatized electrode shows <20% in 60 min. In such experi-mentation it has been demonstrated that each ferrocene center on the surface can be oxidized and reduced >10^5 times without significant loss of electroactive material.(2,3) The decline in efficiency found for n-type Si photoanodes derivatized with II seems to be attributable to the slow growth of an SiO_x layer between the bulk Si and the derivatizing layer.

The ability to observe sustained electrical output from n-type Si-based cells after derivatization of the surface of Si with II indicates that such surface chemistry may prove useful. The maximum value of E_V is 0.5 - 0.6 V for n-type Si derivatized with II which is not too bad considering that the band gap, E_g, of Si is only 1.1 eV. The ferrocene system is fairly durable in both oxidation states and its heterogeneous electron transfer kinetics are good; k_4 is large. Further, the ferricenium does not appear to be capable of effecting Si oxidation to an extent that a thick, insulating SiO_x layer results. Unfortunately, the features that make the ferricenium/ferrocene couple attractive

also detract from its usefulness in the generation of energy-rich compounds using the photoanode-based cells. First, ferricenium is an oxidant, but a weak one; $E^{\circ'}$(ferricenium/ferrocene) for the surface species derived from II is ~+0.5 V vs. SCE. Some data for $E^{\circ'}$ for various electrodes are given in Table I. Second, and more important, ferricenium is a one-electron, outer-sphere oxidant. Most of the desired photoanodic process for fuel formation involve multi-electron transfer processes: O_2 from H_2O, Br_2 from Br^-, etc. Thus, while there are many aqueous reagents B that can be oxidized with a large value of k_5, equation (5), the generation of useful, powerful oxidatants is either thermo-dynamically forbidden or kinetically sluggish. Electrodes only derivatized with II thus do not provide evidence that useful oxidation processes can be effected. However, it may be possible to introduce oxidation catalysts into the derivatizing layer from II that will accelerate the multi-electron processes of interest, as has been done for H_2 evolution, vide infra.(7,8)

Work in other laboratories has demonstrated that n-type Si or GaAs can be protected from photocorrosion using a derivatizing procedure involving the polymerization of pyrrole to coat the surface with an electronically conducting film.(4,5) This procedure is analogous to coating the electrode with a uniform metal overcoat to yield a "buried" photosensitive interface. In such a case, the h^+ does not contact the liquid electrolyte at all and thus photocorrosion is only possible if there are pinholes in the polymer overcoat. As for the surfaces derived from II, the polypyrrole-coated electrodes likely suffer from poor kinetics for processes such as O_2 generation and surface catalysts are needed. Again, however, considerable improvement in durability is attainable compared to naked photoanodes.

Catalysis of H_2 Generation from P-Type Semiconductor Photocathodes

Many p-type semiconductors should be capable of effecting the generation of H_2 from H_2O using light as the driving force, since it can be shown that the bottom of the conduction band, E_{CB}, can be more negative than $E^{\circ'}(H_2O/H_2)$. Work in this laboratory has focused on the use of p-type Si as a photocathode.(7,8) It was shown that N,N'-dimethyl-4,4'-bipyridinium, MV^{2+}, can be photoreduced to MV^+ in aqueous solution at a pH where $E^{\circ'}(MV^{2+/+})$ ~ $E^{\circ'}(H_2O/H_2)$ establishing the interface energetics to be as represented in Scheme III.(21,22) For MV^{2+} reduction to MV^+ the maximum E_V was found to be ~0.5 V. For p-type photocathodes E_V is the extent to which the photoreduction can be effected at a more positive potential than E_{redox} of the redox species. Good photocurrent-voltage curves were found for the p-type Si/$MV^{2+/+}$ system.
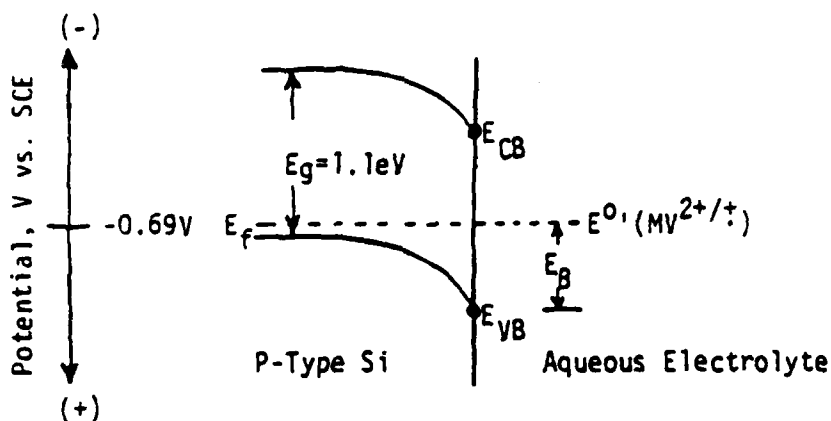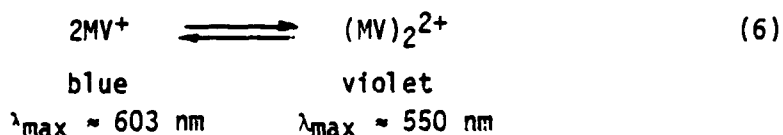
Scheme III. Representation of the interface energetics for p-type Si in contact with an aqueous electrolyte solution containing the $MV^{2+/+}$ couple at its formal potential. The barrier height E_B approximately equals the maximum photovoltage, E_V. The maximum E_V is obtained at high light intensity at open-circuit.

Under the conditions where the MV^{2+} reduction occurs with good output parameters the reduction of H_2O does not occur, despite the fact that formation of MV^+ is as difficult thermo-dynamically as the formation of H_2 from H_2O. Not unexpectedly, the formation of H_2 from H_2O is kinetically more difficult than the one-electron, outer-sphere reduction of MV^{2+}. At this point, work in this laboratory commenced toward the use of reagent III as a derivatizing agent for p-type Si, since the reducing power of the MV^+ is sufficiently great to evolve H_2 from H_2O at pH < 7. Exploiting the reducing power, though, requires the use of a catalyst to equilibrate the ($MV^{2+/+}$) with (H_2O/H_2). Our work has been involved with the use of polymers derived from III that are confined to the p-type Si surface, $[(PQ^{2+} \cdot 2Br^-)_n]_{surf.}$, that have been further functionalized to include either Pt(0) or Pd(0) to equilibrate the $[(PQ^{2+/+})_n]_{surf.}$ with the (H_2O/H_2) couple.

A number of physical techniques have been used to charac-terize electrode surfaces derivatized with III. In the first study (23), the cyclic voltammetry of Pt and p-type Si electrodes bearing $[(PQ^{2+} \cdot 2Br^-)_n]_{surf.}$ was used to confirm the surface attachment of polymeric quantities of PQ^{2+} centers. In CH_3CN/electrolyte solution the positions of waves on Pt for the

$[(PQ^{2+/+})_n]_{surf.}$ and $[(PQ^{+/0})_n]_{surf.}$ systems are very close to those expected from the $E^{\circ\prime}$ for $(MV^{2+/+})$ in solution.(23) Some representative data for the N,N'-dialkyl-bipyridinium systems are given in Table II. Notice that the $E^{\circ\prime}$ for $[(PQ^{2+/+})_n]_{surf.}$ in H_2O electrolyte is somewhat more positive ($\sim$100-150 mV) than the $E^{\circ\prime}$ for the $(MV^{2+/+})$ solution species. We attributed(8) this shift to the fact that the radical monocations of such species are known to reversibly dimerize as shown in equation (6) for the

$$2MV^+ \rightleftharpoons (MV)_2{}^{2+} \qquad\qquad (6)$$

$$\text{blue} \qquad\qquad \text{violet}$$

$$\lambda_{max} \approx 603 \text{ nm} \qquad \lambda_{max} \approx 550 \text{ nm}$$

MV^+ case.(24) Optical spectral changes as a function of the concentration of the MV^+ (or the one-electron reduced form of III)(25) are consistent with the reversible equilibrium represented by equation (6). The $[(PQ^{2+/+})n]_{surf.}$ system is violet in color(25), not blue, consistent with aggregation of the PQ^+ centers due to the high effective concentration. Since the $E^{\circ\prime}$ data for $(MV^{2+/+})$ in H_2O solution are for low concentrations, the $E^{\circ\prime}$ is not directly comparable to that for the surface-confined analogue. These properties (optical spectra and $E^{\circ\prime}$) associated with aggregation of the redox center represent one of the ways that the surface-confined species may depart from expectations from measurements for the solution species at low concentration.

In addition to optical spectra and cyclic voltammetry, Auger spectra and Auger spectra while sputtering surfaces modified with III have been crucial to the development of a surface catalyst for improving H_2 kinetics. For example, recording Auger signal intensity for various elements while sputtering the surface of p-type Si derivatized with III gives an analysis of elemental composition as a function of depth from the outer surface. So-called depth profile analyses yielded the essential representation of the interface given in Scheme IV.(7) A key

P-Type Si   SiO$_x$ $[(PQ^{2+} \cdot 2Br^-)_n]_{surf.}$
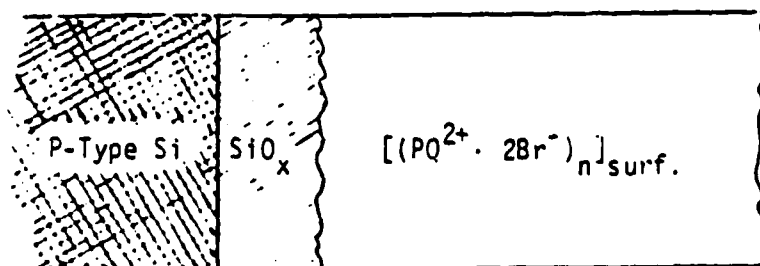
Scheme IV. Side view of the interface resulting from functionalization of p-type Si with reagent III. At about 10^{-8} mol of PQ^{2+} per cm^2 the thickness of the polymer is in the vicinity of 1000 Å.
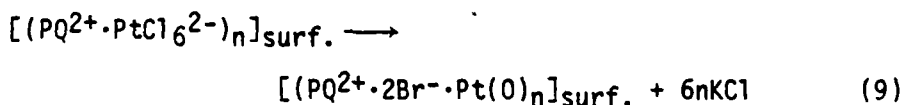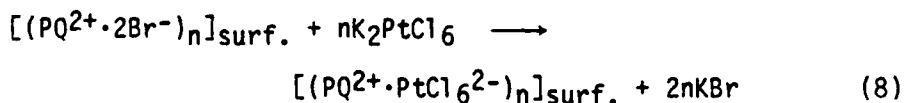
feature revealed is the presence of a SiO_x layer between the bulk p-type Si and the polymer. The oxide is likely the air oxide found on Si and is in the range of 20 Å in thickness and non-stoichiometric.(26,27) The consequence of the non-stoichiometric oxide is that there remains a significant density of surface states at the p-type Si/SiO_x interface such that Fermi level pinning occurs.(13,28)

There is considerable reservation concerning the use of Auger spectroscopy and sputtering techniques for organic materials owing to problems typically encountered from e^- beam and sputtering beam damage.(29) In our system we have been fortunate to be able to test whether there are problems of this sort by using the fact that ion exchange reactions can occur as in equation (7) that lead to the persistent electrostatic binding

$$[(PQ^{2+} \cdot 2Br^-)_n]_{surf.} + nK_2IrCl_6 \rightarrow [(PQ^{2+} \cdot IrCl_6^{2-})_n]_{surf.} + 2nKBr \quad (7)$$
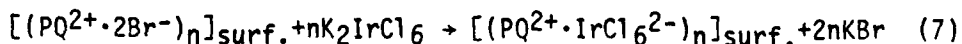
of reversibly electroactive anions as has been done earlier by other workers.(30-32) Analysis of the amount of the electro-active anion present relative to the amount of PQ^{2+} on the surface can be established by cyclic voltammetry. Subsequent analysis of the same surfaces by depth profile analysis reveals excellent consistency with the data from cyclic voltammetry. Table III summarizes Auger and cyclic voltammetry analyses of electrode surfaces bearing PQ^{2+} that were exposed to $H_2O/0.1$ M K_2SO_4/K_2IrCl_6.(33) Note that under the conditions employed, the Ir complex is ultimately present in the polylmer as the $IrCl_6^{3-}$ and that >25 μM $IrCl_6^{2-}$ is sufficient to completely charge compensate the PQ^{2+} system. At low $IrCl_6^{2-}$ concentrations the SO_4^{2-} is competitively bound to the surface and there is an excellent correlation with Cl (from $IrCl_6^{3-}$) Auger signal intensity with the cyclic voltammetry data. A number of such competitive ion binding experiments have given us confidence in the depth profile technique for the substrate/$[(PQ^{2+} \cdot 2X^-)_n]_{surf.}$ systems. We regard Auger signal intensities to give relative elemental composition to $\sim\pm20\%$ for these systems.

The ion exchange reaction represented by equation (7) is directly relevant to our studies of H_2 evolution in that we recognized that the $[(PQ^{2+})_n]_{surf.}$ itself does not react with H_2O to yield H_2 even though such is thermodynamically possible for pH below ~5. Thus, we incorporated Pt(0) into the surface-confined polymer according to equations (8) and (9) in order to

$$[(PQ^{2+} \cdot 2Br^-)_n]_{surf.} + nK_2PtCl_6 \longrightarrow$$

$$[(PQ^{2+} \cdot PtCl_6^{2-})_n]_{surf.} + 2nKBr \qquad (8)$$

$$[(PQ^{2+} \cdot PtCl_6^{2-})_n]_{surf.} \longrightarrow$$

$$[(PQ^{2+} \cdot 2Br^- \cdot Pt(0)_n]_{surf.} + 6nKCl \qquad (9)$$

equilibrate the $[(PQ^{2+/+})_n]_{surf.}$ couple with the (H_2O/H_2) couple. (7,8) Direct evidence that this can be done comes from functionalization of the inside of a Pyrex test tube with III followed by ion exchange with $PtCl_6^{2-}$ and chemical reduction of the surface-confined system with H_2 at pH $\approx$ 7. Reduction of $[(PQ^{2+})_n]_{surf.}$ to $[(PQ^+)_n]_{surf.}$ using H_2 can be monitored spectrophotometrically as a function of pH.(8) In the absence of Pt(0) no detectable reaction occurs. For $[(PQ^{2+/+} \cdot Pt(0))_n]_{surf.}$ we find that the spectral changes with pH under 1 atm H_2 yield an $E^{\circ\prime}$ for the $[(PQ^{2+/+})_n]_{surf.}$ couple that is the same, within experimental error, as that found from cyclic voltammetry.(34)

Photocathode material p-type $Si/[(PQ^{2+} \cdot 2Cl^- \cdot Pt(0))_n]_{surf.}$ does yield much improved H_2 evolution compared to naked p-type Si. In particular, the naked electrode gives no significant photocurrent at E_f more positive than $E^{\circ\prime}(H_2O/H_2)$. This means that there is no output photovoltage for the H_2 evoultion and light (to create carriers) and electrical energy are needed to reduce H_2O. In fact, less total electrical energy would be needed to reduce H_2O with a good conventional H_2 electrode such as platinized Pt. For the derivatized p-type Si photoelectrode we observe that $[(PQ^{2+})_n]_{surf.}$ can be reduced to $[(PQ+)_n]_{surf.}$ under $\geq E_g$ illumination at E_f up to ~0.5 V more positive than $E^{\circ\prime}$ for $[(PQ^{2+/+})_n]_{surf.}$. Thus, at the high light intensity limit we find $E_V \approx 0.5$ V. The incorporation of Pt(0) into the surface polymer thus allows realization of an $E_V \approx 0.5$ V for the reduction of H_2O to H_2. Photocurrent for H_2 evolution from the p-type $Si/[(PQ^{2+} \cdot 2Cl^- \cdot Pt(0))_n]_{surf.}$ onsets at the potential where the reduction of $[(PQ^{2+})_n]_{surf.}$ occurs. Since the $E^{\circ\prime}$ for $[(PQ^{2+/+})_n]_{surf.}$ is essentially independent of pH, Table II, and $E^{\circ\prime}(H_2O/H_2)$ varies 59 mV/pH, there is an optimum pH where rate (current) times E_V is a maximum. Table IV shows some typical sets of power output (photocurrent x E_V) data vs. pH for the p-type $Si/[(PQ^{2+} \cdot 2Cl^- \cdot Pt(0))_n]_{surf.}$ photocathodes. These data are consistent with a mechanism for rate improvement involving first reduction of the $[PQ^{2+}]_{surf.}$ followed by equilibration of the $[(PQ^{2+/+})_n]_{surf.}$ couple with the (H_2O/H_2) couple via the dispersed Pt(0).

The elemental Pt(0) is dispersed throughout the surface polymer as determined by depth profile analysis,(7) and a representation of the interface is given in Scheme V. According

to this view there is a certain amount of Pt(0) in contact with the thin SiO_x overlayer on the bulk p-type Si. This is a relevant structural feature, since direct deposition of Pt(0) onto photocathode surfaces is known to improve the efficiency for the reduction of H_2O to H_2. Thus, we expect that, for an interface like that depicted in Scheme V, there will be a certain
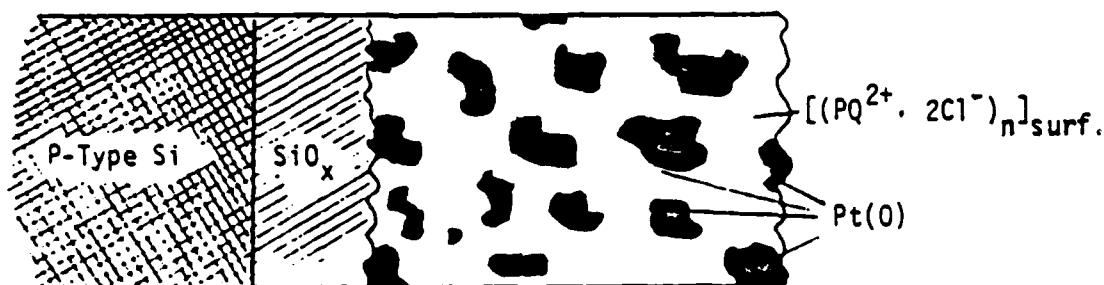

Scheme V. Side view of interface resulting from ion exchange of interface shown in Scheme IV with $PtCl_6^{2-}$ followed by reduction to form Pt(0) dispersed through the polyion.

amount of the H_2 evolution occurring by direct catalysis of the reaction of the photoexcited electrons with H_2O at the SiO_x/Pt(0) interfaces. In the extreme of a uniform, pinhole-free coverage of Pt(0) on p-type Si/SiO_x one expects that the photocathode would operate as a buried photosensitive interface and in fact would be equivalent to an external solid state photovoltaic device driving a photoelectrolysis cell with a Pt(0) cathode. In such a case the maximum power from the device (photocurrent times E_V) would be independent of the pH of the solution. However, for Pt(0) electrochemically deposited onto p-type Si/SiO_x photocathodes in amounts of $\sim 10^{-8}$ mol/cm^2, we find that the output depends on pH such that a lower efficiency is found at the low pH's, Table IV.(7,8) For the p-type Si/SiO_x/Pt(0) photocathodes the pH-efficiency data demand a different mechanism for improvement of efficiency compared to that for p-type $Si/SiO_x/[(PQ^{2+}\cdot2Cl^-\cdot Pt(0))_n]_{surf.}$. The key fact is that the efficiency appears to peak at a particular pH for the redox polymer system, consistent with the pH independent reducing power of the redox couple. For the case of Pt(0) on the p-type Si/SiO_x the efficiency rises from low to high pH and does not show a peak. The fact that there is a pH dependence at all indicates that the photosensitive interface is not completely buried. The Pt(0) can be regarded as a catalyst for the reactions of the excited electrons and does not completely dominate the behavior of the interface with respect to photovoltage.
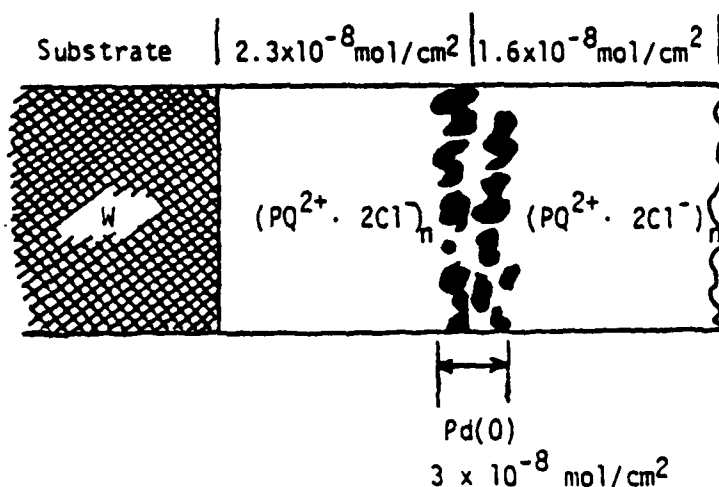
The ambiguity associated with the Pt(0) at the SiO_x in Scheme V has prompted us to synthesize interfaces where the catalyst used to equilibrate the $[(PQ^{2+/+})_n]_{surf.}$ couple with the (H_2O/H_2) couple is not dispersed throughout the polymer.(35) Additionally, to better test the interface structure we have turned to use of Pd(0) instead of Pt(0) as the catalyst. The kinetics for the equilibration of (H_2O/H_2) with Pd(0) are expected to be as good as for Pt(0),(36) but Pd(0) has the advantage of being much more easily detected (~25x more sensitive)(37) by Auger than is Pt(0). This allows better signal to noise in the depth profile analyses used to establish the distribution of catalyst in the polymer.

The interfaces represented by the sketch in Scheme VI have been prepared and characterization by Auger/depth profile analysis is consistent with the preparation procedure.(35) For example, in determining that Pt(0) is distributed throughout the polymer we had no proof that different distributions would yield different depth profiles. Depth profiles for the interfaces represented by Scheme VI do confirm the viability of the use of the technique to determine interface structure. Figure 1 shows representative data for a substrate/$[(PQ^{2+} \cdot 2X^-)_n/Pd(0)/-(PQ^{2+} \cdot 2X^-)_n]_{surf.}$ interface prepared by electrodeposition of the first $(PQ^{2+})_n$ layer by holding the metal electrode at -0.6 V vs. SCE in an aqueous KCl solution of 1 mM III at pH = 7 until the coverage of $[(PQ^{2+} \cdot 2Cl^-)_n]_{surf.}$ equalled 2.3 x 10^{-8} mol/cm^2 from integration of the cyclic voltammogram for the surface-confined material. The electrode was then withdrawn, washed and immersed in aqueous 0.1 M KCl and potentiostatted at -0.6 V vs. SCE to reduce the $[(PQ^{2+})]_{surf.}$ partially to $[(PQ^+)_n]_{surf.}$. While the electrode was held at -0.6 V vs. SCE, K_2PdCl_4 was added to the electrolyte and cathodic current immediately resulted, consistent with reduction of $PdCl_4^{2-}$ to Pd(0). At this point, a depth profile analysis is consistent with a substrate/$[(PQ^{2+} \cdot 2Cl^-)_n/-Pd(0)]_{surf.}$ interface. Electrodeposition of an additional 1.6 x 10^{-8} mol/cm^2 of PQ^{2+} from reduction of III in pH ~ 7 KCl yields the depth profile given in Figure 1 that is consistent with the substrate/$[(PQ^{2+} \cdot 2Cl^-)_n/Pd(0)/(PQ^{2+} \cdot 2Cl^-)_n]_{surf.}$ detailed in Scheme VII.

An electrode such as W/$[(PQ^{2+} \cdot 2Cl^-)_n/Pd(0)/-(PQ^{2+} \cdot 2Cl^-)_n]_{surf.}$ gives improved H_2 evolution properties compared to naked W in that the H_2 overvoltage is reduced.(35) However, the current-voltage curves for such an electrode indicate that the improvement only occurs for pH's where the $[(PQ^{2+/+})_n]_{surf.}$ has the reducing power to reduce H_2O to H_2. It would appear that these findings accord well with the conclusion that the dominant mechanism for H_2 evolution catalysis requires reduction of the $[(PQ^{2+})_n]_{surf.}$. Findings for $[(PQ^{2+} \cdot 2Cl^-)_n/-Pd(0)]_{surf.}$ where the Pd(0) is only on the outermost surface are
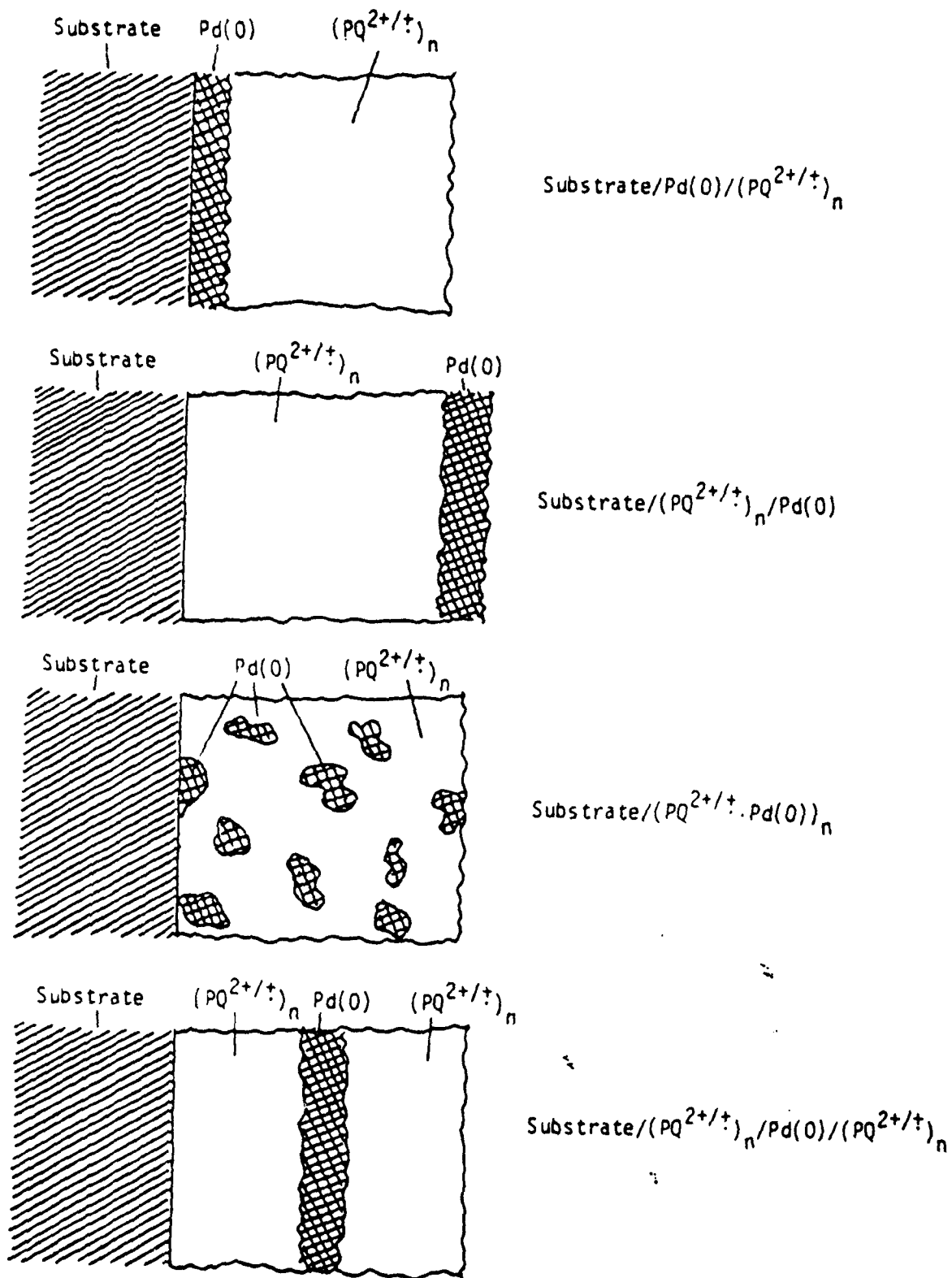
Scheme VI. Representation of interfaces prepared from derivatization of substrates with III and Pd(0). From ref. 35. See also Figures 1 and 3 for Auger depth profile analyses supporting structural assignments.

Substrate | 2.3×10^{-8} mol/cm^2 | 1.6×10^{-8} mol/cm^2 |

$(PQ^{2+} \cdot 2Cl^-)_n$ $(PQ^{2+} \cdot 2Cl^-)_n$

W

Pd(0)

3×10^{-8} mol/cm^2

Scheme VII. Representation of the interface characterized
by the depth profile analysis of Figure 1. Coverages
indicated were determined electrochemically. Data from
reference 35. See text for syntheitic procedures used to
prepare this interface.

also consistent with the mechanism, Figures 2 and 3. These
results fully confirm the conclusion drawn from the earlier
studies(7,8) of the redox polymer/Pt(0) catalyst systems where
Pt(0) is dispersed throughout the polymer.

In our experiments the role of the $[(PQ^{2+})_n]_{surf.}$ is to
rapidly capture the photoexcited electrons; the Pt(0) or Pd(0)
equilibrates the $[(PQ^{2+/+})_n]_{surf.}$ with the (H$_2$O/H$_2$) couple.
Overall, the result is the catalysis of the process represented
by equation (10). All mechanisms for catalysis of this process

$$2e^- + 2H^+ \longrightarrow H_2 \tag{10}$$

can give the same ultimate efficiency. For example, the direct
platinization can improve H$_2$ evolution, Table IV. The
polymer/Pt(0) system should only work well at pH's where the
polymer is a sufficiently good reductant. The directly
platinized surfaces do not have such a pH dependence. It is true

that deliberate manipulation of the polymer can effect changes in the $E°'$ so that the cells could operate at optimum efficiency at other pH's. However, it is not clear that a redox polymer is the procedure of choice to improve H_2 evolution. Direct platini- zation may suffer from the requirement of using a large amount of Pt in order to achieve the buried junction likely needed to achieve durability. At this point, the only safe conclusion is that the redox polymer/Pt(0) or Pd(0) systems do improve H_2 evolution kinetics for cathodes such as illuminated p-type Si or W in the dark. Whether the approach is viable for practical systems is not presently known.

Improvement of Kinetics for Photoreduction of Horseheart Ferri- cytochrome c: A Prototype Example of Superior Properties from Molecular Derivatization

Many biological molecules that can undergo simple, one-electron transfer processes often have very poor electrode kinetics owing in some cases to the fact that the redox center is buried deep inside the macromolecule.(38) However, such reagents sometimes do undergo rapid bimolecular redox reactions with small redox reagents called mediators.(39) For example, horseheart ferricytochrome c, cyt $c_{(ox)}$, is only sluggishly reduced at most electrode surfaces,(40) but cyt $c_{(ox)}$ reacts with MV^+, equation (11), with a very large bimolecular rate constant.(41) This

$$\text{cyt } c_{(ox)} + MV^+ \longrightarrow \text{cyt } c_{(red)} + MV^{2+} \qquad (11)$$
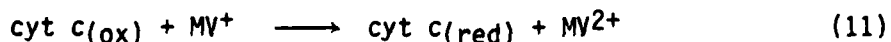
raises the possibility of anchoring known mediators to electrode surfaces for the purpose of improving electron transfer kinetics. In our laboratory reagent III was used to functionalize Au, Pt, or p-type Si surfaces for the purpose of illustrating this principle.(6)

The reversible systems Au or $Pt/[(PQ^{2+} \cdot 2Br^-)_n]_{surf}$. were shown to be superior electrodes for cyt $c_{(ox)}$ reduction compared to the naked electrodes.(6) Reduction of cyt $c_{(ox)}$ was found to be mass transport limited when the electrode potential was held sufficiently negative to reduce the $[(PQ^{2+})_n]_{surf}$. to $[(PQ^+)_n]_{surf}$. Thus, the results accord well with a mechanism where the reduction of cyt $c_{(ox)}$ occurs in a mass transport limited reaction with surface-confined PQ^+ centers.

P-type Si photocathodes functionalized with III also effect the reduction of cyt $c_{(ox)}$ with superior kinetics compared to the naked electrode.(6) The naked p-type Si does not effect the reduction at a significant rate. The illuminated p-Si/- $[(PQ^{2+} \cdot 2Br^-)_n]_{surf}$. cathode can be used to effect the reduction of cyt $c_{(ox)}$ at a potential ~0.5 V more positive than at Au or Pt, consistent with the value of E_V for the $[(PQ^{2+/+})_n]_{surf}$. system, Table II.

It is important to recognize that $E^{\circ\prime}$ for $(MV^{2+/+})$ or $[(PQ^{2+/+})_n]_{surf.}$ is significantly more negative than $E^{\circ\prime}(cyt$ $c_{(ox)}/cyt \ c_{(red)}) = +0.02$ V vs. SCE.(42) In terms of practical consequence this means that the reversible electrodes, Au or Pt, do not respond to $(cyt \ c_{(ox)}/cyt \ c_{(red)})$ at the thermodynamic potential. To do this requires a surface-confined mediator having an $E^{\circ\prime}$ in the vicinity of that for the cyt c̲ system while preserving the large rate constants.

The data for illuminated p-type Si indicate that reduction of cyt $c_{(ox)}$ can be effected at more positive potentials, but the objective would be to obtain a good value of E_V with respect to the biological couple. Again this requires a better match of the $E^{\circ\prime}$ of the surface mediator with that of the biological reagent. It is known that the $(MV^{2+/+})$ system is a mediator system for a large number of biological redox systems including enzymes capable of catalyzing important multielectron transfer reactions.(43) Future studies may take advantage of the redox polymer systems to equilibrate the biological catalysts with the oxidizing and reducing carriers created by absorption of light by semiconductor electrodes. However, the practical consequences will remain small unless the photoelectrodes can be shown to have sufficiently good efficiency for the redox reaction of the mediator system. For example, the E_V of ~0.5 V for the $p-Si/[(PQ^{2+}\cdot 2X^-)_n]_{surf.}$ system (Table II) is too low to give high efficiency. The E_V for $p-InP/[(PQ^{2+}\cdot 2Cl^-)_n]_{surf.}$ system is ~0.8 V but there appear to be greater problems with interface stability.(44,45) In any event, surface attachment of mediators would appear to be a rational approach to equilibrating biological redox agents with conductors and is an area where the molecular derivatization procedure is promising. Unlike H_2 evolution that can be improved by direct platinization or corrosion that can be suppressed by overcoats of electronically conducting material, the equilibration of biological redox substances with surfaces will likely require the molecular approach.

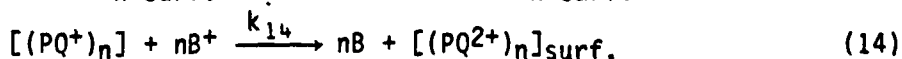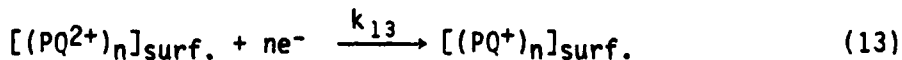## Measurement of Electron Transfer Rate Constants Involving Surface-Confined Redox Reagents

Semiconductor electrodes provide an excellent substrate for the study of redox reactions of surface-confined redox reagents. This follows from the fact that the ratio of oxidized to reduced form of a redox couple on a photoelectrode responds to two stimuli, light and potential, rather than to only potential as is the case for a redox couple confined to a reversible electrode. For example, the generation of surface-confined ferricenium from ferrocene on n-type Si requires $>E_g$ illumination and an electrode potential that is sufficiently positive. The oxidation of ferrocene does not occur in the dark, but the reduction of

ferricenium will occur provided the electrode potential is moved sufficiently negative because there are plenty of majority charge carriers avilable. Thus, we have used the two stimuli response to determine rate constants such as k_5 of equation (5).(9,10) The measurement involves the determination of the time dependence of the surface concentration of A^+ = ferricenium in the presence of B and as a function of the concentration of B. The concentration of the surface oxidant is easily measured in the dark after reaction time t_i by a rapid potential sweep to a potential where the surface ferricenium is reduced, equation (12). Integration

$$\text{surface-ferricenium} + e^- \longrightarrow \text{surface-ferrocene} \qquad (12)$$
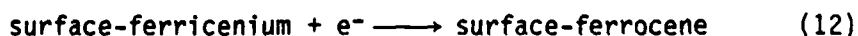
of the current associated with equation (12) gives the remaining surface-ferricenium concentration. The experiment is possible on a semiconductor photoanode and not on a reversible electrode because once the ferricenium is photogenerated and illumination terminated there will be no additional ferricenium generated. By way of contrast, a reversible electrode will always have a ratio of oxidized to reduced material on the surface that is dependent only on the potential. For the photoanode the surface oxidant can be reduced by a solution reductant in the dark and the reaction can be monitored electrochemically. For n-type Si electrodes functionalized with I or II, measurements of k_5 have been performed. The data show that equations (4) and (5) can account for 100% of the photocurrent. The data rule out any significant component of electrocatalysis not involving a redox reaction of a surface-ferricenium and a solution reductant. Further, the variation in k_5 with B accords well with expectations from self-exchange rates of (B^+/B) couples, the self-exchange rate of (ferricenium/ferrocene), and the driving force of reaction.(9,10)

Similarly, rate constants for reaction of photogenerated surface reductants on p-type semiconductors can be measured. Thus, for the p-type Si electrodes derivatized with III, we are concerned with processes represented by equations (13) and (14).

$$[(PQ^{2+})_n]_{surf.} + ne^- \xrightarrow{k_{13}} [(PQ^+)_n]_{surf.} \qquad (13)$$

$$[(PQ^+)_n] + nB^+ \xrightarrow{k_{14}} nB + [(PQ^{2+})_n]_{surf.} \qquad (14)$$

For B^+ = cyt $c_{(ox)}$ we have examined the time dependence of the surface concentration of $[(PQ^+)_n]_{surf.}$ in the dark.(6) We find that the oxidation of $[(PQ^+)_n]_{surf.}$ is limited by the rate of mass transport of cyt $c_{(ox)}$ up to the surface, consistent with data for reduction at rotating disk $Pt/[(PQ^{2+/+})_n]_{surf.}$ electrodes. Again, the direct electrochemical measurement of the time dependence of the surface concentration of PQ^+ allows the conclusion that the mechanism for cyt $c_{(ox)}$ reduction only

involves a redox mediation and no other surface catalysis, such
as that observed by other workers(46,47) for other systems, need
be invoked in the case. It is the ability to directly electro-
chemically monitor surface concentrations of the redox reagent
that makes the semiconductor surface unique compared to
reversible electrode surfaces. This allows an assessment of
mechanism and predictability of redox reactivity from theory and
measurements involving solution species.

At this point, it is worth noting that polymer-coated
electrodes may suffer from a problem associated with charge
transport through the polymer. For example, the reduction of
$Ru(NH_3)_6^{3+}$ according to equation (15) has been studied at

$$[(PQ^+)_n]_{surf.} + nRu(NH_3)_6^{3+} \xrightarrow{k_{15}}$$

$$[(PQ^{2+})_n]_{surf.} + nRu(NH_3)_6^{2+} \qquad (15)$$
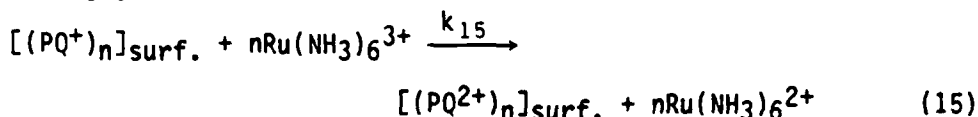
rotating disk $[(PQ^{2+} \cdot 2Cl^-)_n]_{surf.}$ electrodes.(8) For coverages
of ~10^{-8} mol/cm^2 it appears thaat linear plots of cathodic
current vs. $\omega^{1/2}$ can be obtained only up to certain current
densities, ~20 mA/cm. This limit depends on the concentration of
the supporting KCl electrolyte and decreases with decreasing KCl
concentration. These data are consistent with the conclusion
that current is ultimately limited by charge transport in the
polymer. This limitation may be quite important in practical
applications and requires additional studies. For example,
current densities of >20 mA/cm^2 could be expected for an
efficient solar photoelectrochemical device. Transport of ions
and electrons must both be fast in order to overcome this
limitation even if the specific rate constants such as k_5, k_{14},
or k_{15} are sufficiently large.

Alteration of Interface Energetics and Surface States by Chemical Modification

Semiconductor electrodes modified with reagents I-III
exhibit properties that are fairly well predicted from the
properties associated with the naked semiconductors in contact
with ferrocene or MV^{2+}. Strongly interacting modifiers may alter
the interface energetics and surface state distribution in useful
ways.(11-14) A classic example of altering surface state
distribution comes from electronic devices based on Si.(48) The
semiconducting Si has a large density of surface states situated
between the valence band and the conduction band. Oxidation of
the surface to produce a Si/SiO$_x$ interface results in a
substantial diminution of the states between the valence and
conduction band edges of the Si, but the density of surface
states depends on the surface chemistry. Another example of
surface state alteration may be the example of the improvement of

output parameters for n-type GaAs-based photoelectrochemical devices from surface pretreatment of n-type GaAs with $RuCl_3$.([14]) Recent results in this laboratory have shown that oxidizing etches for pretreating n-type CdTe can yield a Te-rich overlayer on the surface resulting in Fermi level pinning.([49,50]) A reducing etch pretreatment can lead to an n-type CdTe photoanode having nearly ideal variation of the barrier height, E_B, with changes in E_{redox} of the solution, Figure 4.([49]) These examples illustrate possible consequences of semiconductor surface modification not encountered with molecular reagents. These sorts of modification would appear to be crucial to practical achievements, since interface states will likely control e^- - h^+ recombination rates and E_V. Thus, controlled modification of semiconductor surfaces will be needed to achieve the high efficiency required in solar energy devices.

Ion adsorption to an electrode surface can also be regarded as a type of surface modification that can have a profound effect on photoelectrochemistry.([11,12]) A classic example here is the pH dependence of the band edge positions of metal oxide electrodes.([51]) Recently, work in this laboratory has illustrated that ion adsorption can dramatically alter the photoelectrochemical performance of a semiconductor.([11]) It was shown that the presence of as little as 1 mM I^- in 6 M H_2SO_4/1 M SO_2 can alter the band edge positions of WS_2 as illustrated in Schemne VIII.
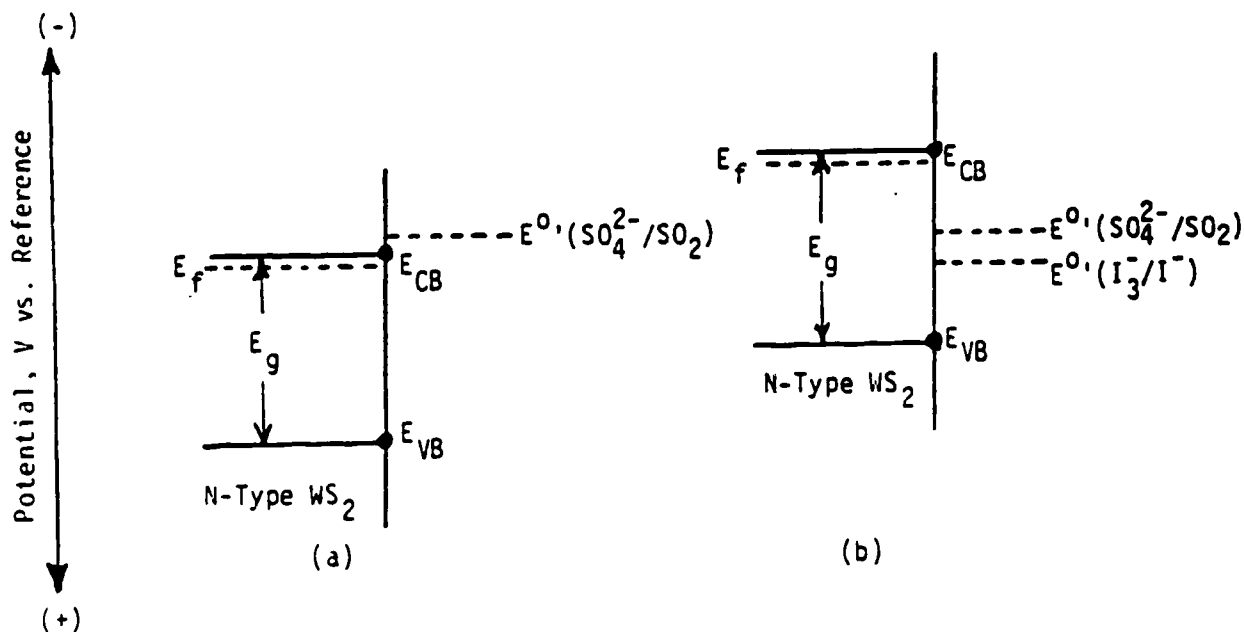
Scheme VIII. Interface energetics for n-type WS_2 in the absence (a) and presence of I^- in H_2SO_4/SO_2 solution. Data are from ref. 11.

The ~0.6 V negative shift allows a fairly good E_V to be obtained with respect to $E^{o'}(SO_4^{2-}/SO_2)$. Further, the photooxidation of the I^- significantly improves the overall rate of SO_2 oxidation via equations (16) and (17). In the absence of I^- the

$$3I^- + 2h^+ \longrightarrow I_3^- \tag{16}$$

$$2H_2O + SO_2 + I_3^- \longrightarrow SO_4^{2-} + 3I^- + 4H^+ \tag{17}$$
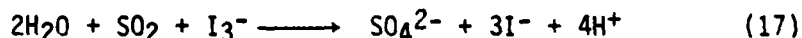
$E^{\circ\prime}(SO_4^{2-}/SO_2)$ indicates that SO_2 oxidation should occur in the dark, since E_{CB} is more positive. However, SO_2 oxidation has poor kinetics(52), and oxidation of the SO_2 is not found either in the dark or upon $>E_g$ illumination. The I^- thus plays the dual role of favorably altering the interface energetics (to give a good E_V) and providing a mechanism to give good kinetics. Figure 5 illustrates the effect of I^- on the photoelectrochemical oxidation of SO_2 at illuminated MoS_2 that behaves in a manner similar to that for WS_2.(11) The n-type WS_2 is able to effect the overall process represented by equation (18). The H_2 is evolved at the dark cathode and the process can be effected with

$$2H_2O + SO_2 \xrightarrow[\text{I^- catalyst}]{>1.3 \text{ eV light}} H_2SO_4 + H_2 \tag{18}$$
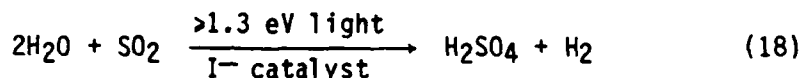
no energy input other than the light. At ~50% H_2SO_4 the process is ~0.3 V uphill(52) and the surprisingly rugged n-type WS_2 gives 632.8 nm power conversion efficiencies of up to ~13% (~6 mW/cm^2 input) with no other energy input.

Ions are not typically persisitently bound and their lability may preclude general utility. However, the WS_2/I^- system provides evidence that modification of the proper sort can yield extraordinary consequences. Modification procedures resulting in an irreversible interface change like that from I^- adsorption would be useful.

Conclusion

Chemical treatment of the surfaces of semiconductor photo-electrode surfaces can result in profound, positive changes in interface properties and overall performance of the photo-electrodes. Illustrations of the use of one-electron surface reagents to suppress photocorrosion and to improve electrode kinetics for large biological molecules establishes a possible role for such species in future studies and possibly in applications. However, the important overall processes in photoelectrochemical energy conversion are multi-electron processes that will likely require reagents that involve inner sphere redox character. Combinations such as the redox polymer/-Pt(0) are prototype electron transfer catalysts that can improve kinetics for multi-electron transfer processes. Surface modification to remove surface states and alter interface energetics requires elaboration in order to achieve high efficiency devices. At this point it appears that chemical pretreatments of photo-electrode surfaces will be the rule rather than the exception. The procedures will range from etches for increasing surface area to molecular derivatization for improvement of the rate of equilibration of large biological redox systems with the semi-conductor surface.

Acknowledgements

TABLE I. Formal Potentials and Photovoltages for
Surface-Confined Ferrocene Reagents

Derivatizing Reagent	Electrode Substrate	$E^{\circ\prime}$, V vs. SCE $\pm$ 0.03[a]	E_V, V[b]
I	Pt	+0.43	---
	Au	+0.43	---
	n-type Si	[+0.43][c]	~0.4 - 0.6
II	Pt	+0.50	---
	Au	+0.45	---
	n-type Si	[+0.45][c]	~0.5 - 0.6
	n-type GaAs	[+0.45][c]	~0.7
	n-type Ge	[+0.45][c]	~0.2

[a]Data for Pt and Au electrodes are from cyclic voltammograms in CH_3CN/0.1 M [n-Bu$_4$N]Cl0$_4$. Data are from a number of determinations as given in: Wrighton, M.S.; Palazzotto, M.C.; Bocarsly, A.B.; Bolts, J.M.; Fischer, A.B.; Nadjo, L. J. Am. Chem. Soc., 1978, 100, 7264; Bolts, J.M.; Wrighton, M.S. ibid., 1978, 100, 5257 and 1979, 101, 6179; Bruce, J.A.; Wrighton, M.S. J. Electroanal. Chem., 1981, 122, 93; Fischer, A.B. Ph.D. Thesis, M.I.T., 1981.

[b]E_V is the photovoltage obtained for the derivatized n-type semiconductor photoanodes. We assume $E^{\circ\prime}$ to be the values given in brackets and E_V is the extent to which the peak of the photoanodic current is more negative than $E^{\circ\prime}$ under >E_g illumination. Data are from references given in (a).

[c]We assume $E^{\circ\prime}$ to be the same on the n-type semiconductors as on metallic electrodes but these values have not been measured, since the n-type semiconductors generally are not reversible.

Table II. Formal Potentials and Photovoltages for Surface-
Confined N,N'-Dialkyl-4,4'-Bipyridinium Reagents and
For Solution N,N'-Dimethyl-4,4'-Bipyridinium

Species[a]	Electrode	Solvent	$E^{\circ\prime}$,V vs. SCE[b]	E_V, V[c]
$(MV^{2+/+})_{soln.}$	Pt,Au,n-Si	CH_3CN	-0.45	---
	p-Si	CH_3CN	[-0.45][d]	~0.5
	p-InP	CH_3CN	[-0.45][d]	~0.8[e]
	Hg, n-Si	H_2O(pH=1-7)	-0.69	---
	Pt, Au	H_2O(pH=7)	-0.69	---
	p-Si	H_2O(pH=1-7)	[-0.69][d]	~0.5
	p-InP	H_2O(pH=1-7)	[-0.69][d]	~0.8[e]
$(III)_{soln.}$	Pt,Au,n-Si	CH_3CN	-0.45	---
	Pt,Au,n-Si	H_2O(pH=7)	-0.66	---
$[(PQ^{2+/+})_n]_{surf.}$	Pt,Au,n-Si	CH_3CN	-0.45	---
	Pt,Au,n-Si	H_2O(pH=7)	-0.55	---
	W, n-MoS$_2$			
	p-Si	CH_3CN	[-0.45][d]	~0.5
	p-Si	H_2O(pH=1-7)	[-0.45][d]	~0.5

[a]MV^{2+}=N,N'-Dimethyl-4,4'-bipyridinium; $(III)_{soln.}$ is the species
(III) dissolved in solution; in H_2O, of course, III hydrolyzes;
$[(PQ^{2+/+})_n]_{surf.}$ is the surface-confined material from function-
alization with III.
[b]Data are from ref. 8 and are from the average position of the
reduction and oxidation wave of cyclic voltammetry scans.
[c]E_V is the photovoltage obtained from the p-type semiconductors
for the reduction of the oxidized form of the redox couple. We
assume $E^{\circ\prime}$ to be the values in brackets and E_V is the extent to
which the cathodic current peak is more positive than $E^{\circ\prime}$ under
>E_g illumination.
[d]We assume $E^{\circ\prime}$ to be the same at the p-type semiconductors as on
the reversible electrodes, but these values have not been
measured because the p-type semiconductors are not reversible.
[e]These data from Dominey, R.N.; Lewis, N.S.; Wrighton, M.S.
J. Am. Chem. Soc., 1981, 103, 1261.

Table III. Correlation of Auger and Cyclic Voltammetric
Analysis of $Pt/[(PQ^{2+}\cdot 2/3xIrCl_6^{3-}\cdot(1-x)SO_4^{2-})_n]_{surf.}$[a]

		Cyclic Voltammetry			
Electrode Number	$[K_2IrCl_6]$, μM[b]	Coverage[c] $[(PQ^{2+/+})_n]_{surf.}$	Coverage[c] $[IrCl_6^{3-}]_{surf.}$	x[d]	Auger Cl/C[e]
1	0	5.0×10^{-9}	0	0.0	0
2	1.0	7.6×10^{-9}	0.5×10^{-9}	0.1	0.04
3	2.5	7.6×10^{-9}	1.1×10^{-9}	0.2	0.15
4	5.0	5.0×10^{-9}	1.8×10^{-9}	0.5	0.35
5	25.0	7.3×10^{-9}	3.9×10^{-9}	0.8	0.55
6	50.0	7.3×10^{-9}	5.1×10^{-9}	1.0	0.73

[a] Data are from ref. 33.

[b] K_2IrCl_6 is present at various concentrations indicated; K_2SO_4 is present at 0.1 M in H_2O.

[c] Coverage determined by integration of cyclic voltammetry waves for $[(PQ^{2+/+})_n]_{surf.}$ and then for $[IrCl_6^{2-/3-}]_{surf.}$ after equilibration. Units are mol/cm^2 and error is $\pm 5\%$.

[d] x is the stoichiometric coefficient determined by the ratio of the coverage of $[(PQ^{2+})]_{surf.}$ and electrostatically bound $IrCl_6^{3-}$. x ranges from 0-1 in $[(PQ^{2+}\cdot 2/3xIrCl_6^{3-}\cdot(1-x)SO_4^{2-})_n]_{surf.}$.

[e] Auger data are from surface analysis after withdrawing the electrode and washing with distilled H_2O. Data given are the observed relative signal intensity and are not corrected for element sensitivity. C is constant and associated with $[(PQ^{2+})_n]_{surf.}$ and Cl is associated with bound $IrCl_6^{3-}$. Ratios are $\sim \pm 20\%$.

Table IV. Comparison of pH Dependence on Photoelectrochemical H_2 Generation Efficiency from p-Type Si/Pt(0) and from p-Type Si/$[(PQ^{2+} \cdot 2Cl^{-} \cdot Pt(0))_n]_{surf.}$ Photocathodes.[a]

Electrode[b]		pH	Input Pwr at 632.8 nm, mW/cm^2	η,%[c]
p-Si/Pt(0)				
	#1	1.1	11.8	0.4
		3.9	11.8	2.3
		6.5	11.8	4.1
	#2	1.1	11.8	3.5
		3.9	11.8	6.9
		5.4	11.8	7.1
p-Si/$[(PQ^{2+}/2Cl^{-} \cdot Pt(0))_n]_{surf.}$				
	#1	1.0	10.9	0.9
		4.0	10.8	5.0
		5.5	11.2	1.8
	#2	1.0	6.9	1.8
		4.0	6.9	3.8
		8.0	6.9	2.3
	#3	1.0	20.8	0.5
		4.0	20.8	3.7
		5.5	20.8	2.7

[a]Data are from ref. 8.
[b]Electrodes p-Si/Pt(0) have been prepared by electrodeposition of Pt(0) from $PtCl_6^{2-}$ directly onto p-Si/SiO_x; approximate coverage is ~5 x 10^{-8} mol/cm^2. The p-Si/$[(PQ^{2+} \cdot 2Cl^{-} \cdot Pt(0))_n]_{surf.}$ electrodes were prepared by first treating with III followed by ion exchange with $PtCl_6^{2-}$ and reduction to yield Pt(0) dispersed in the polymer. The coverage of PQ^{2+} is typically 10^{-8} mol/cm^2; the ion exchange incorporates one Pt atom per PQ^{2+} center.
[c]Power conversion efficiency. The input power is that from a He/Ne laser (632.8 nm). The output power is E_V times photocurrent. Thus η in % is given by (output power/input power) x100%. Data given are representative of a number of determinations given in ref. 8.

LITERATURE CITED

1. Wrighton, M.S.; Austin, R.G.; Bocarsly, A.B.; Bolts, J.M.; Haas, O.; Legg, K.D.; Nadjo, L.; Palazzotto, M.C. J. Am. Chem. Soc., 1978, 100, 1602.

2. Bolts, J.M.; Bocarsly, A.B.; Palazzotto, M.C.; Walton, E.G.; Lewis, N.S.; Wrighton, M.S. J. Am. Chem. Soc., 1979, 101, 1378.

3. Bocarsly, A.B.; Walton, E.G.; Wrighton, M.S. J. Am. Chem. Soc., 1980, 102, 3390.

4. (a) Noufi, R.; Tench, D.; Warren, L.F. J. Electrochem. Soc., 1980, 127, 2310; (b) Noufi, R.; Frank, A.J.; Nozik, A.J. J. Am. Chem. Soc., 1981, 103, 1849; (c) Skotheim, T.; Lundstrom, I.; Prejza, J. J. Electrochem. Soc., 1981, 128, 1625.

5. Fan, F.-R. F.; Wheeler, B.L.; Bard, A.J.; Noufi, R.N. J. Electrochem. Soc., 1981, 128, 2042.

6. Lewis, N.S.; Wrighton, M.S. Science, 1981, 211, 944.

7. Bookbinder, D.C.; Bruce, J.A.; Dominey, R.N.; Lewis, N.S.; Wrighton, M.S. Proc. Natl. Acad. Sci., U.S.A., 1980, 77, 6280.

8. Dominey, R.N.; Lewis, N.S.; Bruce, J.A.; Bookbinder, D.C.; Wrighton, M.S. J. Am. Chem. Soc., 1982, 104, 0000.

9. Lewis, N.S.; Bocarsly, A.B.; Wrighton, M.S. J. Phys. Chem., 1980, 84, 2033.

10. Lewis, N.S.; Wrighton, M.S. ACS Symposium Series, 1981, 146, 37 "Photoeffects at Semiconductor-Electrolyte Interfaces", A.J. Nozik, ed.

11. Calabrese, G.S.; Wrighton, M.S. J. Am. Chem. Soc., 1981, 103, 6273.

12. Ginley, D.S.; Butler, M.A. J. Electrochem. Soc., 1978, 125, 1968.

13. Bard, A.J.; Bocarsly, A.B.; Fan, F.-R.F.; Walton, E.G.; Wrighton, M.S. J. Am. Chem. Soc., 1980, 102, 3671.

14. Heller, A.; Lewerenz, H.J.; Miller, B. Ber. Bunsenges. Phys. Chem., 1980, 84, 592.

15. Bard, A.J.; Wrighton, M.S. J. Electrochem. Soc., 1977, 124, 1706.

16. Gerischer, H. J. Electroanal. Chem., 1977, 82, 133.

17. Park. S.M.; Barber, M.E. J. Electroanal. Chem., 1977, 99, 67.

18. Wrighton, M.S. Accs. Chem. Res., 1979, 12, 303.

19. Heller, A. Accs. Chem. Res., 1981, 14, 154.

20. Legg, K.D.; Ellis, A.B.; Bolts, J.M.; Wrighton, M.S. Proc. Natl. Acad. Sci., U.S.A., 1977, 74, 4116.

21. Bookbinder, D.C.; Lewis, N.S.; Bradley, M.G.; Bocarsly, A.B.; Wrighton, M.S. J. Am. Chem. Soc., 1979, 101, 7721.

22. Bocarsly, A.B.; Bookbinder, D.C.; Dominey, R.N.; Lewis, N.S.; Wrighton, M.S. J. Am. Chem. Soc., 1980, 102, 3683.

23. Bookbinder, D.C.; Wrighton, M.S. J. Am. Chem. Soc., 1980, 102, 5123.

24. Kosower, E.M.; Cotter, J.L. J. Am. Chem. Soc., 1964, 85, 5524.

25. Bookbinder, D.C.; Wrighton, M.S., to be submitted to J. Electrochem. Soc.

26. Schmidt, P.F.; Michel, W.J. J. Electrochem. Soc., 1957, 104, 230.

27. Raider, S.I.; Flitsch, R.; Palmer, M.J. J. Electrochem. Soc., 1975, 122, 413.

28. McGill, T.C. J. Vac. Sci. Technol., 1974, 11, 935.

29. Davis, R.E.; Faulkner, J.R. J. Electrochem. Soc., 1981, 128, 1349.

30. Oyama, N.; Anson, F.C. J. Electrochem. Soc., 1980, 127, 247, and Anal. Chem., 1980, 52, 1192.

31. Shigerhara, K.; Oyama, N.; Anson, F.C. Inorg. Chem., 1981, 20, 518.

32. Oyama, N.; Sato, K.; Matsuda, H. J. Electroanal. Chem., 1980, 115, 149.

33. Bruce, J.A.; Wrighton, M.S. J. Am. Chem. Soc., 1982, 104, 0000.

34. Bookbinder, D.C.; Lewis, N.S.; Wrighton, M.S. J. Am. Chem. Soc., 1981, 103, 7656.

35. Bruce, J.A.; Murahashi, T.; Wrighton, M.S. J. Phys. Chem., 1982, 86, 0000.

36. Bockris, J. O'M.; Reddy, A.K.N. "Modern Electrochemistry", Vol. 2, Plenum: New York, 1970, p. 1238.

37. Davis, L.E.; MacDonald, N.C.; Palmberg, P.W.; Riach, G.E.; Weber, R.G. "Handbook of Auger Electron Spectroscopy", 2nd ed., Physical Electronics Division, Perkin-Elmer Corp., Eden Prairie, MN, 1972.

38. Margoliash, E.; Schejter, A. in "Advances in Protein Chemistry", Vol. 21, Chap. 2, Anfinsen, C.B.; Edsall, J.T.; Richards, F.M.,eds., Academic Press: New York, 1966.

39. Kuwana, T.; Heineman, W.R. Accs. Chem. Res., 1976, 9, 241.

40. (a) Kono, T.; Nakamura, S. Bull. Agric. Chem. Soc. Jpn., 1958, 22, 399; (b) Haladjian, J.; Bianco, P.; Serve, P.A. J. Electroanal. Chem., 1979, 104, 555; (c) Betso, S.R.; Klapper, M.H.; Anderson, L.B. J. Am. Chem. Soc., 1972, 84, 8197.

41. Land, E.J.; Swallow, A.J. Ber. Bunsenges. Phys. Chem., 1975, 79, 436.

42. Margalit, R.; Schejter, A. Eur. J. Biochem., 1973, 32, 492.

43. Summers, L.A. "The Bipyridinium Herbicides", Academic Press: London, 1980, pp. 122-124.

44. Dominey, R.N.; Lewis, N.S.; Wrighton, M.S. J. Am. Chem. Soc., 1981, 103, 1261.

45. Dominey, R.N.; Wrighton, M.S., to be submitted.

46. Eddowes, M.J.; Hill, H.A.O.; Uosaki, J. J. Am. Chem. Soc., 1979, 101, 7113.
47. Landrum, H.L.; Salmon, R.T.; Hawkridge, F.M. J. Am. Chem. Soc., 1977, 99, 3154.
48. Sze, S.M. "Physics of Semiconductor Devices", Wiley: New York, 1969.
49. Tanaka, S.; Bruce, J.A.; Wrighton, M.S. J. Phys. Chem., 1981, 85, 0000.
50. Aruchamy, A.; Wrighton, M.S. J. Phys. Chem., 1980, 84, 2848.
51. Morrison, S.R. "Electrochemistry at Semiconductor and Oxidized Metal Electrodes", Plenum: 1980.
52. Lu, P.W.T.; Ammon, R.L. J. Electrochem. Soc., 1980, 127, 2610.

Figure Captions

Figure 1. Auger depth profile analysis of a W electrode deriva-
tized first with III, then with Pd(0), and again with III to
yield W/[(PQ^{2+}·2Cl$^-$)$_n$/Pd(0)/(PQ^{2+}·2Cl$^-$)$_n$]$_{surf.}$ after removal from
0.1 M KCl solution as described in the text. The Auger
instrument is a Physical Electronics Model 590A employing a 5 KeV
e$^-$ beam with a beam current of 0.5 to 1 μA. Sputtering was done
using a 2 KeV Ar$^+$ beam from a Physical Electronics Model 04-303
ion gun. Auger signals monitored were: Pd (330 eV); C (272 eV);
and W (1736 eV).

Figure 2. Photocurrent-voltage curves (10 mV/s) for a p-type
Si/[(PQ^{2+}·2Cl$^-$)$_n$/Pd(0)]$_{surf.}$ photocathode where Pd(0) is
deposited only on the outer surface of the redox polymer. The
illumination source is a He-Ne lasaer, 632.8 nm, at ~10 mW/cm^2,
and the exposed electrode area is ~0.1 cm^2. The inset shows the
power conversion efficiency peaking at ~pH = 4. Steady state
photocurrent corresponds to H$_2$ evolution. Data are from ref. 35.

Figure 3. Comparison of pH dependence on H$_2$ evolution for two
different interfaces one where the derivatization with III is
followed by Pd(0) deposition, (a), and one where Pd(0) deposition
directly onto W is followed by derivatization with III, (b). In
(a), only when [(PQ^{2+})$_n$]$_{surf.}$ is reduced is current for H$_2$
observed; in (b) H$_2$ evolution shows the usual 59 mV/pH shift
expected. The insets show Auger depth profile analyses after the
electrodes were used. Data from ref. 35.

Figure 4. Representation of effect from different pretreatment procedures for n-type CdTe. Data points are the photovoltage, E_V, at high light intensity vs. the E_{redox} of the contacting redox couple. The oxidizing etch was 4 g $K_2Cr_2O_7$, 10 ml conc. HNO_3 and 20 ml H_2O into which the n-CdTe was dipped for 30 s at 25°C. The reducing etch pretreatment is to first use the oxidizing etch followed by immersing the n-CdTe into boiling 2.5 $\underline{M}$ NaOH/0.6 $\underline{M}$ $Na_2S_2O_4$ for 3 min. Data are from ref. 49.

Figure 5. Effect of I⁻ adsorption onto n-type MoS_2 on the photoelectrochemical oxidation of 1 $\underline{M}$ SO_2 in 6 $\underline{M}$ H_2SO_4. In the absence of I⁻, (a), no dark or photooxidation of SO_2 occurs. In the presence of 1 m$\underline{M}$ I⁻ the mediated oxidation of SO_2 occurs at a potential corresponding to the onset for I⁻ oxidation. The electrode (0.07 cm^2) was irradiated at 632.8 nm (~40 mW/cm^2). Data are from ref. 11.

Relative Auger Signal Intensity

a) $W/(PQ^{2+})_n/Pd(0)$

b) $W/Pd(0)/(PQ^{2+})_n$

a) n-MoS₂
6 M H₂SO₄

saturated
with SO₂

50 μA

Argon
purged

dark

b) n-MoS₂
6 M H₂SO₄

saturated
with SO₂

100 μA

1.0 mM I⁻

dark

CURRENT

cathodic O anodic

cathodic O anodic

POTENTIAL, V vs. SCE

-0.2   0.0   0.2   0.4   0.6
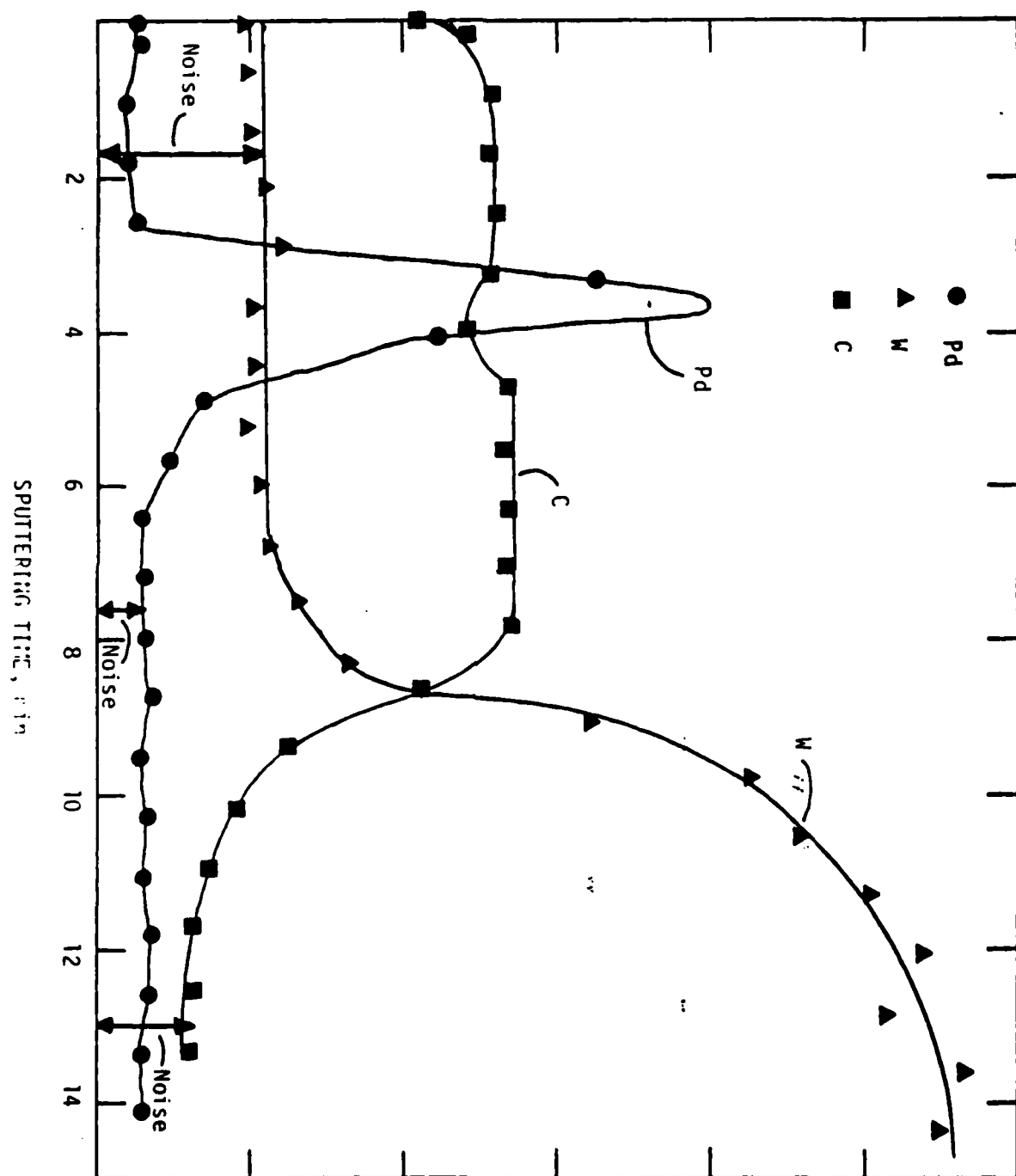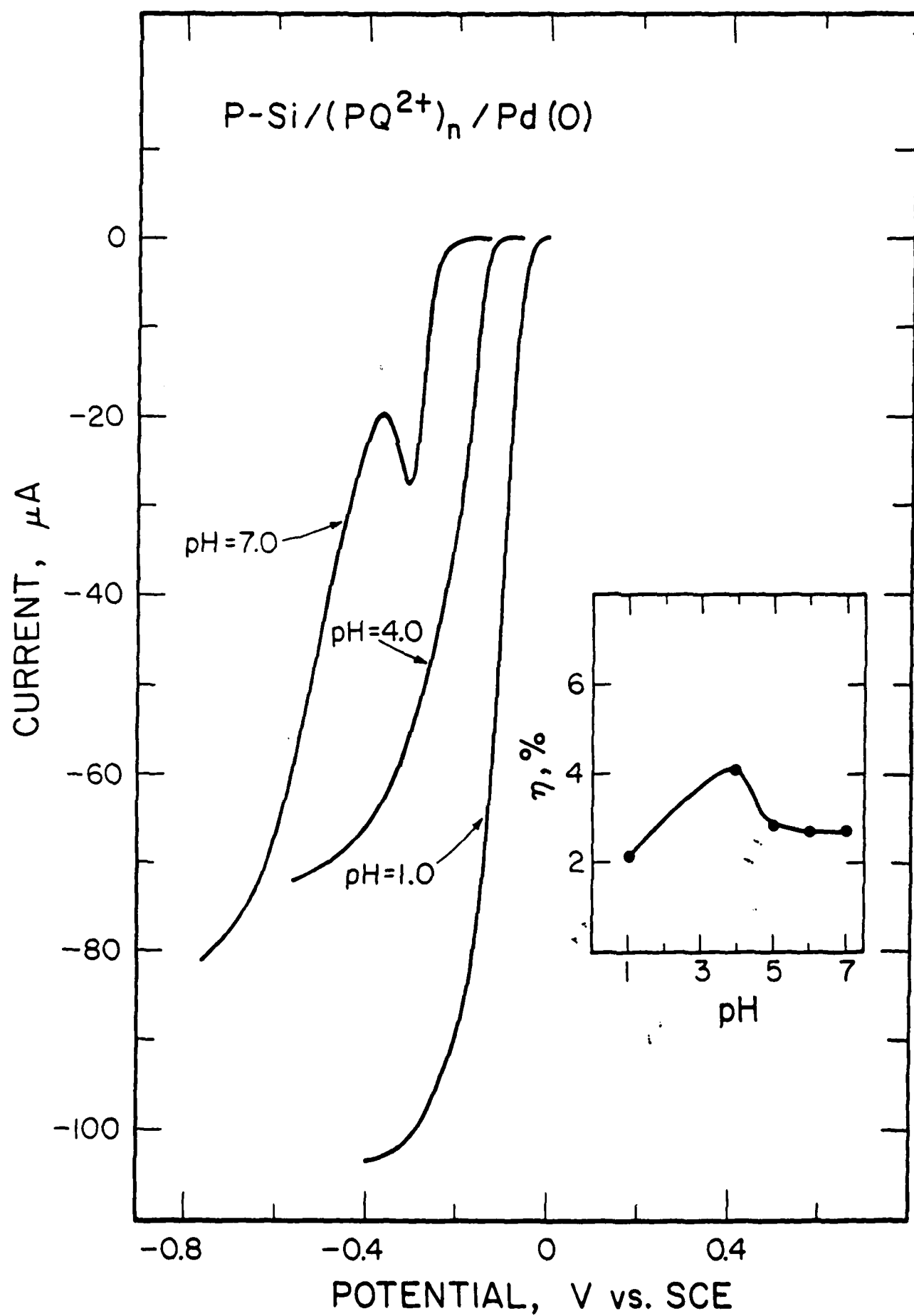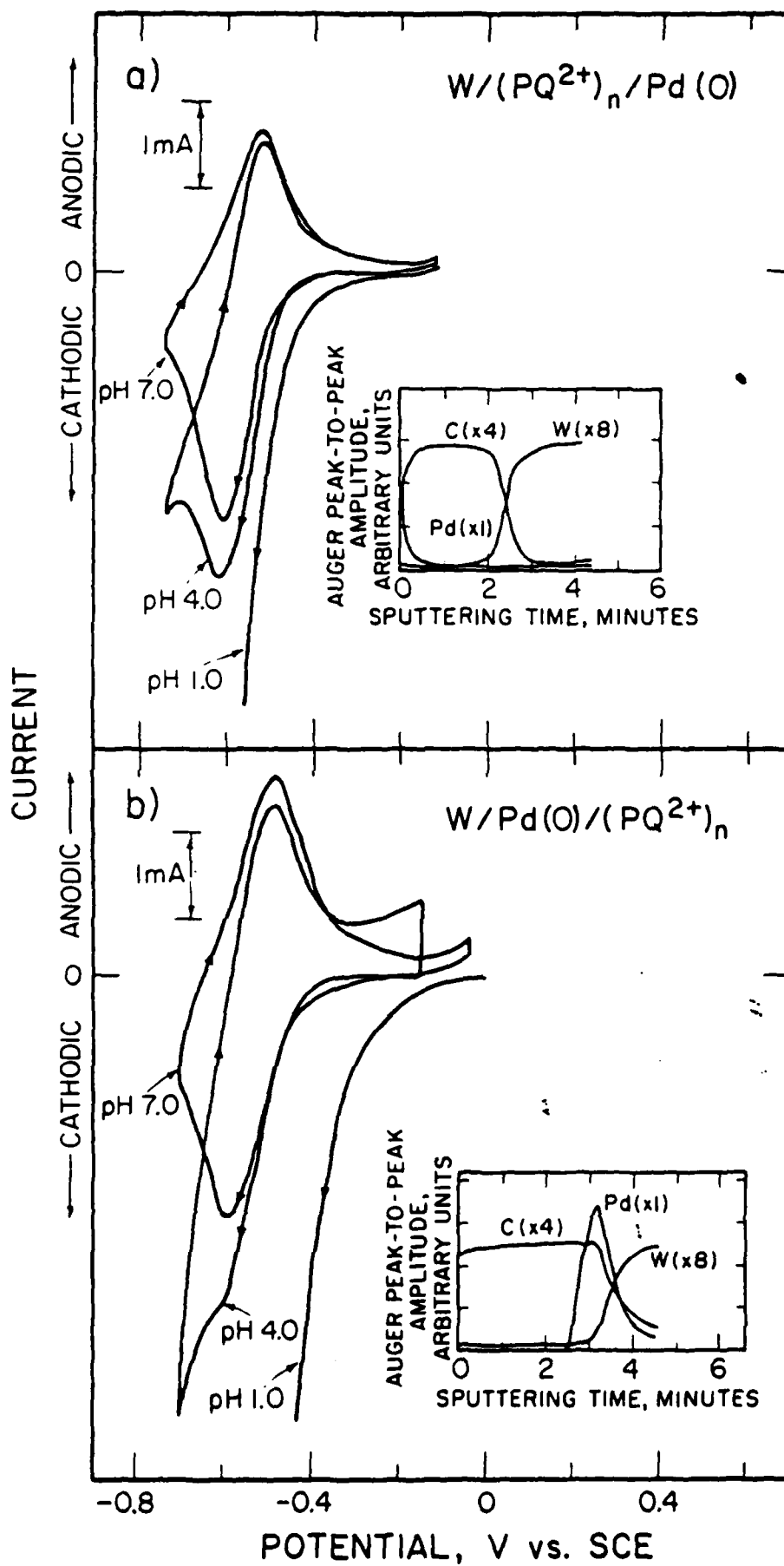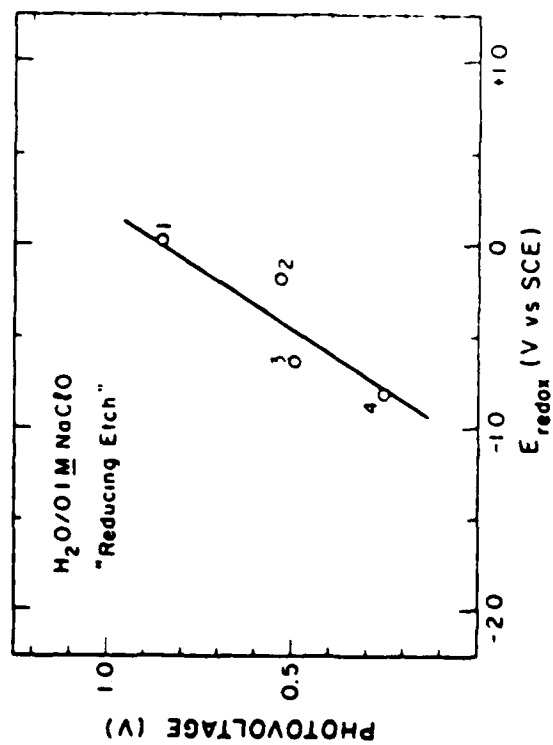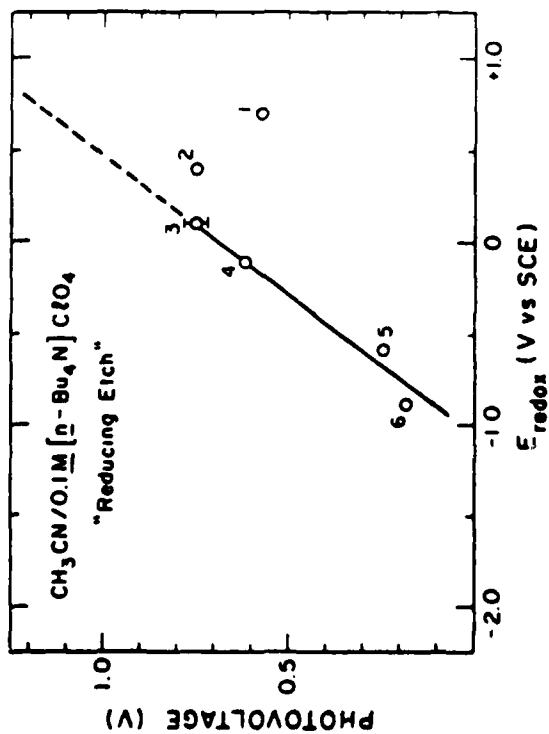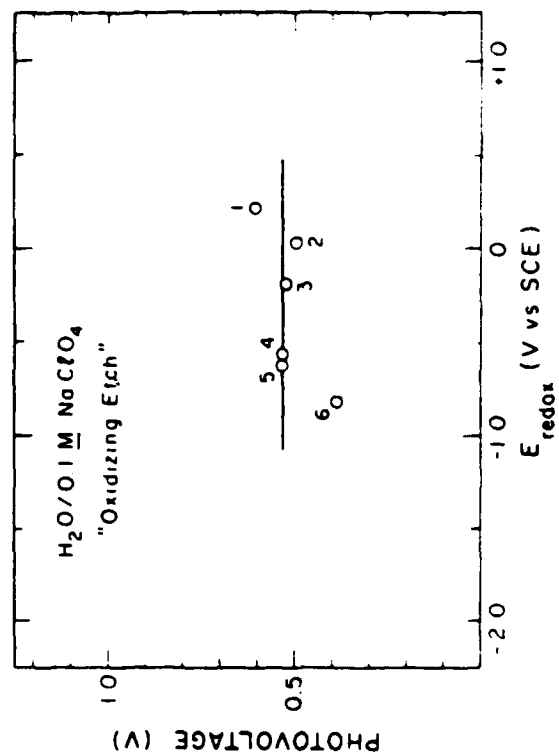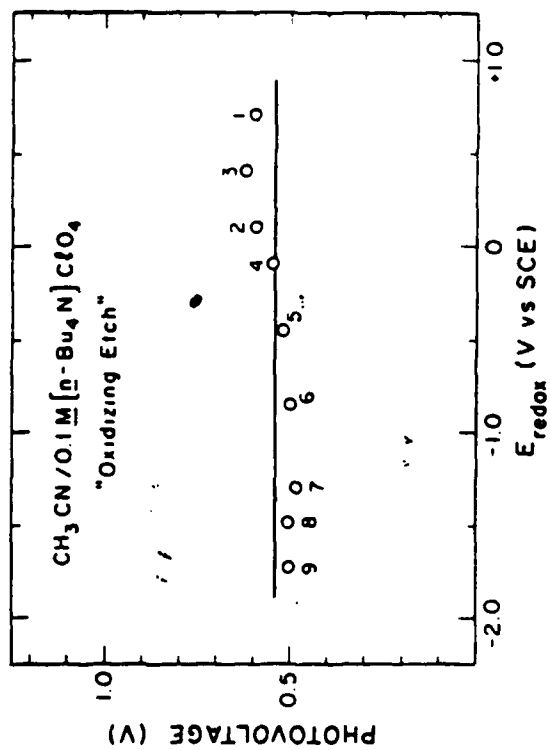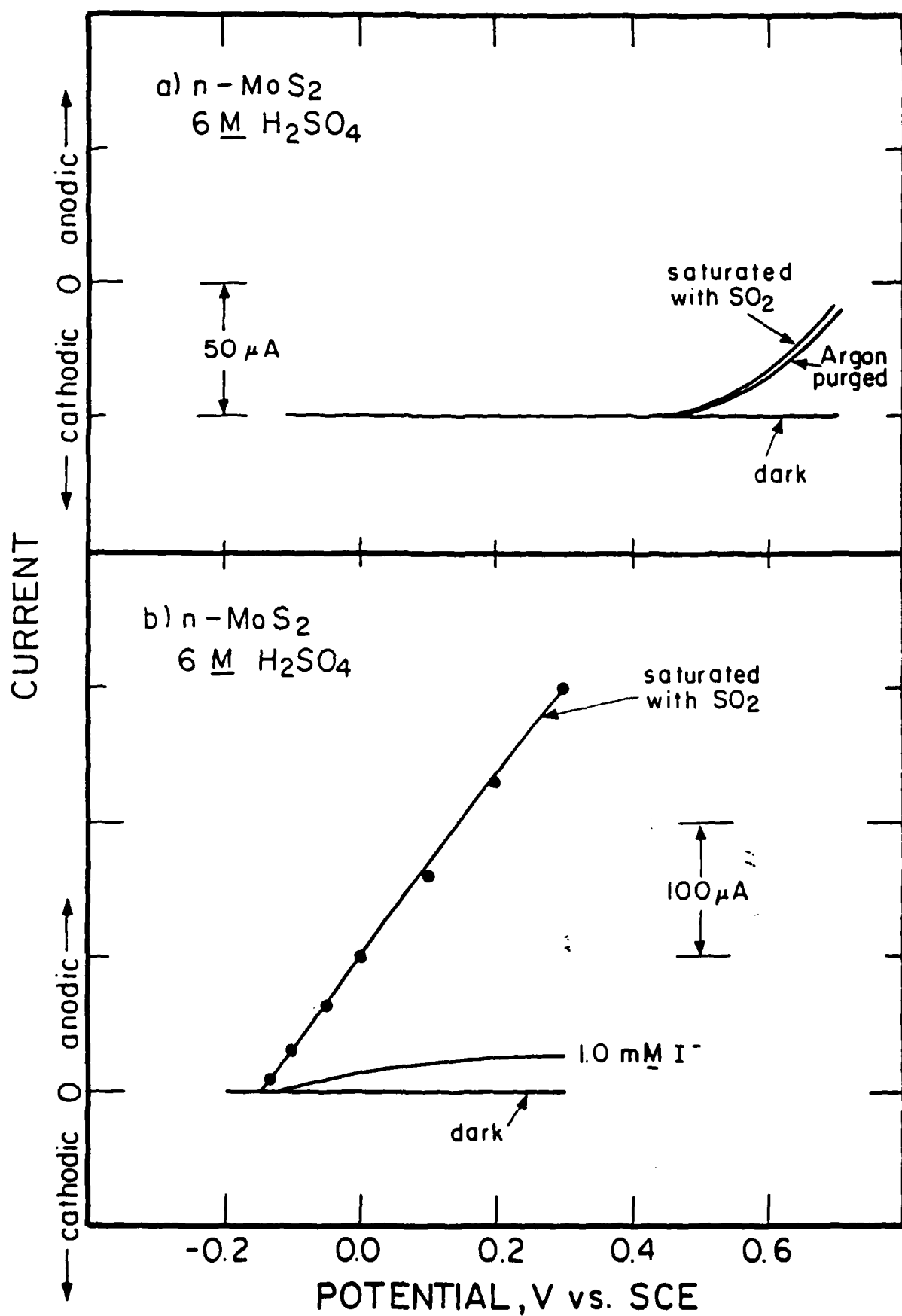
TECHNICAL REPORT DISTRIBUTION LIST, GEN

	No. Copies		No. Copies
Office of Naval Research Attn: Code 472 800 North Quincy Street Arlington, Virginia 22217	2	U.S. Army Research Office Attn: CRD-AA-IP P.O. Box 1211 Research Triangle Park, N.C. 27709	1
ONR Branch Office Attn: Dr. George Sandoz 536 S. Clark Street Chicago, Illinois 60605	1	Naval Ocean Systems Center Attn: Mr. Joe McCartney San Diego, California 92152	1
~~ONR Area Office~~ ~~Discontinued~~ ~~715 Broadway~~ ~~New York, New York 10003~~	1	Naval Weapons Center Attn: Dr. A. B. Amster, Chemistry Division China Lake, California 93555	1
ONR Western Regional Office 1030 East Green Street Pasadena, California 91106	1	Naval Civil Engineering Laboratory Attn: Dr. R. W. Drisko Port Hueneme, California 93401	1
ONR Eastern/Central Regional Office Attn: Dr. L. H. Peebles Building 114, Section D 666 Summer Street Boston, Massachusetts 02210	1	Department of Physics & Chemistry Naval Postgraduate School Monterey, California 93940	1
Director, Naval Research Laboratory Attn: Code 6100 Washington, D.C. 20390	1	Dr. A. L. Slafkosky Scientific Advisor Commandant of the Marine Corps (Code RD-1) Washington, D.C. 20380	1
The Assistant Secretary of the Navy (RE&S) Department of the Navy Room 4E736, Pentagon Washington, D.C. 20350	1	Office of Naval Research Attn: Dr. Richard S. Miller 800 N. Quincy Street Arlington, Virginia 22217	1
Commander, Naval Air Systems Command Attn: Code 310C (H. Rosenwasser) Department of the Navy Washington, D.C. 20360	1	Naval Ship Research and Development Center Attn: Dr. G. Bosmajian, Applied Chemistry Division Annapolis, Maryland 21401	1
Defense Technical Information Center Building 5, Cameron Station Alexandria, Virginia 22314	12	Naval Ocean Systems Center Attn: Dr. S. Yamamoto, Marine Sciences Division San Diego, California 91232	1
Dr. Fred Saalfeld Chemistry Division, Code 6100 Naval Research Laboratory Washington, D.C. 20375	1	Mr. John Boyle Materials Branch Naval Ship Engineering Center Philadelphia, Pennsylvania 19112	1

TECHNICAL REPORT DISTRIBUTION LIST, GEN

No.
Copies

Dr. Rudolph J. Marcus
Office of Naval Research
Scientific Liaison Group
American Embassy
APO San Francisco 96503   1

Mr. James Kelley
DTNSRDC Code 2803
Annapolis, Maryland 21402   1

TECHNICAL REPORT DISTRIBUTION LIST, 359

	No. Copies		No. Copies
Dr. Paul Delahav Department of Chemistry New York University New York, New York 10003	1	Dr. P. J. Hendra Department of Chemistry University of Southhampton Southhampton SO9 5NH United Kingdom	1
Dr. E. Yeager Department of Chemistry Case Western Reserve University Cleveland, Ohio 41106	1	Dr. Sam Perone Department of Chemistry Purdue University West Lafayette, Indiana 47907	1
Dr. D. N. Bennion Department of Chemical Engineering Brigham Young University Provo, Utah 84602	1	Dr. Royce W. Murrav Department of Chemistry University of North Carolina Chapel Hill, North Carolina 27514	1
Dr. R. A. Marcus Department of Chemistry California Institute of Technology Pasadena, California 91125	1	Naval Ocean Systems Center Attn: Technical Library San Diego, California 92152	1
Dr. J. J. Auborn Bell Laboratories Murray Hill, New Jersey 07974	1	Dr. C. E. Mueller The Electrochemistry Branch Materials Division, Research & Technology Department Naval Surface Weapons Center	
Dr. Adam Heller Bell Laboratories Murray Hill, New Jersey 07974	1	White Oak Laboratory Silver Spring, Maryland 20910	1
Dr. T. Katan Lockheed Missiles & Space Co, Inc. P.O. Box 504 Sunnyvale, California 94088	1	Dr. G. Goodman Globe-Union Incorporated 5757 North Green Bay Avenue Milwaukee, Wisconsin 53201	1
Dr. Joseph Singer, Code 302-1 NASA-Lewis 21000 Brookpark Road Cleveland, Ohio 44135	1	Dr. J. Boechler Electrochimica Corporation Attention: Technical Library 2485 Charleston Road Mountain View, California 94040	1
Dr. B. Brummer EIC Incorporated 55 Chapel Street Newton, Massachusetts 02158	1	Dr. P. P. Schmidt Department of Chemistry Oakland University Rochester, Michigan 48063	1
Library P. R. Mallory and Company, Inc. Northwest Industrial Park Burlington, Massachusetts 01803	1	Dr. H. Richtol Chemistry Department Rensselaer Polytechnic Institute Troy, New York 12181	1

TECHNICAL REPORT DISTRIBUTION LIST, 359

	No. Copies		No. Copies
Dr. A. B. Ellis Chemistry Department University of Wisconsin Madison, Wisconsin 53706	1	Dr. R. P. Van Duyne Department of Chemistry Northwestern University Evanston, Illinois 60201	1
~~Dr. M. Wrighton~~ ~~Chemistry Department~~ ~~Massachusetts Institute~~ ~~of Technology~~ ~~Cambridge, Massachusetts 02139~~	1	Dr. B. Stanley Pons Department of Chemistry University of Alberta Edmonton, Alberta CANADA T6G 2G2	1
Larry F. Plew Naval Weapons Support Center Code 30736, Building 2906 Crane, Indiana 47522	1	Dr. Michael J. Weaver Department of Chemistry Michigan State University East Lansing, Michigan 48824	1
S. Ruby DOE (STOR) 600 E Street Washington, D.C. 20545	1	Dr. R. David Rauh EIC Corporation 55 Chapel Street Newton, Massachusetts 02158	1
Dr. Aaron Wold Brown University Department of Chemistry Providence, Rhode Island 02192	1	Dr. J. David Margerun Research Laboratories Division Hughes Aircraft Company 3011 Malibu Canyon Road Malibu, California 90265	1
Dr. R. C. Chudacek McGraw-Edison Company Edison Battery Division Post Office Box 28 Bloomfield, New Jersey 07003	1	Dr. Martin Fleischmann Department of Chemistry University of Southampton Southampton 509 5NH England	1
Dr. A. J. Bard University of Texas Department of Chemistry Austin, Texas 78712	1	Dr. Janet Ostervoung Department of Chemistry State University of New York at Buffalo Buffalo, New York 14214	1
Dr. M. M. Nicholson Electronics Research Center Rockwell International 3370 Miraloma Avenue Anaheim, California	1	Dr. R. A. Ostervoung Department of Chemistry State University of New York at Buffalo Buffalo, New York 14214	1
Dr. Donald W. Ernst Naval Surface Weapons Center Code R-33 White Oak Laboratory Silver Spring, Maryland 20910	1	Mr. James R. Moden Naval Underwater Systems Center Code 3632 Newport, Rhode Island 02840	1

TECHNICAL REPORT DISTRIBUTION LIST, 359

	No. Copies		No. Copies
Dr. R. Nowak Naval Research Laboratory Code 6130 Washington, D.C. 20375	1	Dr. John Kincaid Department of the Navy Stategic Systems Project Office Room 901 Washington, DC 20376	1
Dr. John F. Houlihan Shenango Valley Campus Pennsylvania State University Sharon, Pennsylvania 16146	1	M. L. Robertson Manager, Electrochemical Power Sonices Division Naval Weapons Support Center Crane, Indiana 47522	1
Dr. M. G. Sceats Department of Chemistry University of Rochester Rochester, New York 14627	1	Dr. Elton Cairns Energy & Environment Division Lawrence Berkeley Laboratory University of California Berkeley, California 94720	1
Dr. D. F. Shriver Department of Chemistry Northwestern University Eva ston, Illinois 60201	1	Dr. Bernard Spielvogel U.S. Army Research Office P.O. Box 12211	
Dr. D. H. Whitmore Department of Materials Science Northwestern University Evanston, Illinois 60201	1	Research Triangle Park, NC 27709	1
Dr. Alan Bewick Department of Chemistry The University Southampton, S09 5NH England	1	Dr. Denton Elliott Air Force Office of Scientific Research Bldg. 104 Bolling AFB Washington, DC 20332	1
Dr. A. Himv NAVSEA-5433 NC #4 2541 Jefferson Davis Highway Arlington, Virginia 20362	1		

TECHNICAL REPORT DISTRIBUTION LIST, 051A

	No. Copies		No. Copies
Dr. M. A. El-Sayed Department of Chemistry University of California, Los Angeles Los Angeles, California 90024	1	Dr. M. Rauhut Chemical Research Division American Cyanamid Company Bound Brook, New Jersey 08805	1
Dr. E. R. Bernstein Department of Chemistry Colorado State University Fort Collins, Colorado 80521	1	Dr. J. I. Zink Department of Chemistry University of California, Los Angeles Los Angeles, California 90024	1
Dr. C. A. Heller Naval Weapons Center Code 6059 China Lake, California 93555	1	Dr. D. Haarer IBM San Jose Research Center 5600 Cottle Road San Jose, California 95143	1
Dr. J. R. MacDonald Chemistry Division Naval Research Laboratory Code 6110 Washington, D.C. 20375	1	Dr. John Cooper Code 6130 Naval Research Laboratory Washington, D.C. 20375	1
Dr. G. B. Schuster Chemistry Department University of Illinois Urbana, Illinois 61801	1	Dr. William M. Jackson Department of Chemistry Howard University Washington, DC 20059	1
Dr. A. Adamson Department of Chemistry University of Southern California Los Angeles, California 90007	1	Dr. George E. Walraffen Department of Chemistry Howard University Washington, DC 20059	1
Dr. M. S. Wrighton Department of Chemistry Massachusetts Institute of Technology Cambridge, Massachusetts 02139	1		